# Pickering emulsions stabilized by stimuli-responsive microgels: study of their stability

**Auteur :** Duggal, Hitesh
**Promoteur(s) :** Pfennig, Andreas
**Faculté :** Faculté des Sciences appliquées
**Diplôme :** Cours supplémentaires destinés aux étudiants d'échange (Erasmus, ...)
**Année académique :** 2021-2022
**URI/URL :** http://hdl.handle.net/2268.2/14174

# Pickering emulsions stabilized by stimuli-responsive microgels: study of their stability

Master's thesis to obtain the academic master's degree of

**Advanced Materials: Innovative Recycling**

submitted to

**Université de Liège (Faculty of Applied Sciences)**

By: Hitesh Duggal

Supervisors:

Dr. Véronique Schmitt: Researcher, Centre de Recherche Paul Pascal, CNRS, France

Dr. Valérie Ravaine: Professor, INP Bordeaux, France,

Dr.-Ing. Andreas Pfennig: Professor, Department of Chemical Engineering at University of Liège, Belgium

Liège, Belgium

June 2022

Academic year 2021-2022

## Acknowledgment

Firstly, and most importantly, I would like to thank, Dr. Cécile Zakri, director of the CRPP (Centre de Recherche Paul Pascal) and Dr. Philippe Garrigues, director of the ISM (Institut des Sciences Moléculaires) for allowing me to do this internship in their establishments.

I would like to thank my supervisors, Dr. Veronique Schmitt and Dr. Valérie Ravaine, for their assistance and support throughout the project, as well as for welcoming me to their respective labs. I am also grateful to Magdalena Przeradzka for her advice and guidance offered throughout the internship. I would like to thank Eric Laurichesse for technical support with various instrumentation used during the internship.

Finally, I would also like to acknowledge all the team of the laboratory: the teachers-researchers, the PhD students, the trainees and various members of staff at the CRPP and ISM who helped welcome me into the lab and offered support at various stages.

# Table of Contents

## Table of Figures

# Abstract

Emulsions are a type of dispersing system that consists of two liquids that are incompatible with one another. Emulsions can be made stable by employing microgels (so-called Pickering emulsions) as stabilizers. Microgel-stabilized emulsions have unique features because of the rigidity of the surfaces as microgels are soft and deformable colloidal particles that are swollen by a solvent and exhibit the capacity to deform and adsorb at liquid interfaces. This study aims to comprehend the relationship between the parameters influencing the interfacial properties of emulsions and their mechanical behavior. The first section of the result addressed the formation of emulsions by means of rotor stator homogenization that is driven by limited coalescence phenomenon. Then, the compression behavior of the emulsions was determined by measuring the relationship between osmotic pressure and droplet's volume fraction after they are centrifuged and examined the effect of microgel's cross-linking density and their size, the nature of the oil phase, as well as formulation process (emulsification procedure) on the emulsion's flocculation state and compression behavior. The results were interpreted in terms of the elasticity of the adsorbent particles due to the presence of intrinsically attractive contacts, which proved that the interface of microgels-stabilized drops exhibits the linear relationship between stress and strain that is typical of elastic behavior. As a result, small size microgels of the 2.5% BIS type appeared to be the most suitable for obtaining non-flocculated and kinetically stable emulsions with the highest osmotic pressure and droplets volume fraction as well as linear behavior in interpretation which confirmed the elastic behavior of the emulsion.



Keywords: Pickering Emulsions, Microgels, Interfaces, Deformable Particles, Flocculation, Stabilization, Limited Coalescence, Compression, Osmotic Pressure, Droplet Volume Fraction, Elasticity

# I Introduction and State of the Art

## 1. Emulsions

An emulsion is a fluid colloidal system in which liquid droplets and/or liquid crystals are dispersed in a liquid. The droplets often exceed the usual limits for colloids in size. The dispersion medium correlates to the fluid present as colloidal particles, whereas the continuous phase corresponds to a second liquid that is immiscible with the first. When the continuous phase is water, the emulsion called an oil-in-water (O/W) emulsion. Once the continuous phase is oily, the emulsion is a water-in-oil (W/O) mixture (Figure 1) as defined by IUPAC [1].


**Figure 1: Representation of oil-in-water emulsion (left) and water-in-oil emulsion (right) [72]**

Emulsions can remain kinetically stable for a long period, which is what decides how long they can be stored. They are, nevertheless, inherently unstable in the thermodynamic sense meaning the energy fundamental state. Emulsions may nevertheless remain stable for a long period of time, which is known as metastability. Stabilizers, which in this case are surfactants, can be used to increase the system's kinetic stability. Because they are amphiphilic, these substances are one of a kind (i.e., one-part a polar and lipophilic, the other polar and hydrophilic). As a result of their attraction for oil and water, they can adsorb at the oil-water interface of emulsion drops. To stabilize the emulsion, the free energy of the interfacial area is reduced by the presence of the

emulsifiers at the interface. When stabilizing an emulsion, surfactants aren't the only option. Polymers and even particles are examples of alternatives [2] [3].

## 2. Pickering Emulsions

Solid colloidal particles help to stabilize dispersed systems of two incompatible liquids. Unlike ordinary emulsions, these emulsions do not contain surfactants known as emulsifying agents. This phenomenon is known as Pickering Emulsion. Ramsden was the first to report on the long-term stabilization of oil-in-water emulsions by particles in 1903 [4] and then the research was conducted by S.U. Pickering for knowing more important characteristics of Pickering Emulsions in 1907 [5]. Pickering emulsions are currently generating fresh interest, as illustrated in Figure 2.

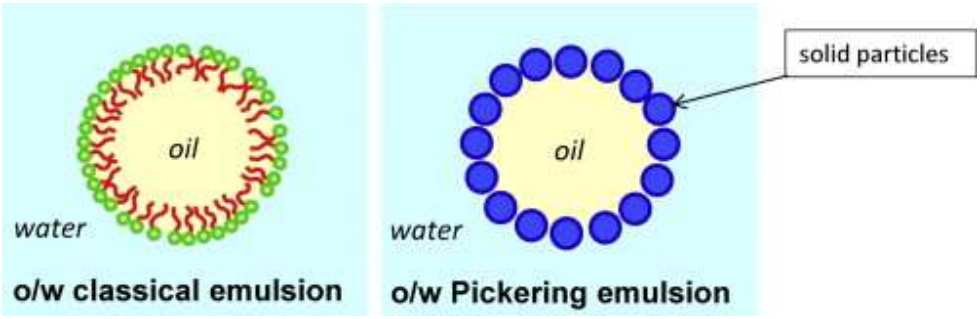


**Figure 2: Representation of Pickering Emulsions [6]**

Compared with traditional emulsions stabilized by surfactants, Pickering emulsions are advantageous in the following four aspects:

1. Emulsions are easy to prepare [2]
2. Less emulsifier is needed, therefore saving the cost. [3]
3. Solid particles are less harmful to human bodies and the environment relative to surfactants. [3]
4. The formed emulsions are very stable and insensitive to the pH, salinity, temperature, and oil composition of the system. [3]

Surfactant-free characteristics make them interesting for a variety of applications where surfactants can have unwanted consequences (irritation, hemolytic behavior, etc.) [2] [3] [6] [7]. As an additional benefit, they are more stable than other emulsions. Droplets are protected from coalescence by a dense film that forms around them because the solid particles that have adhered to the oil-water interface are non-reversible. This is in contrast to emulsions, in which a thermodynamic equilibrium is present between the surfactant molecules in solution and surfactant molecules that are adsorbed at the oil-water interface. Due to the irreversible particle adsorption (see 3.3), Pickering emulsions are remarkably kinetically stable.

In comparison to conventional emulsions stabilized by surfactants, Pickering emulsions have seen renewed interest since the beginning of the 2000s because of their extremely favorable qualities from an application point of view as shown in Figure 3. Due to the advantages (e.g., higher stability and lower toxicity) of solid particles relative to surfactant-based emulsions, the number of studies on Pickering emulsions has increased significantly in recent years because of the potential value of these emulsions for different and novel applications due to their "surfactant-free" quality that makes them suitable particularly in industry (i.e., food technology, cosmetic products, oil recovery and, more recently, drug delivery. [3] [6] [7]

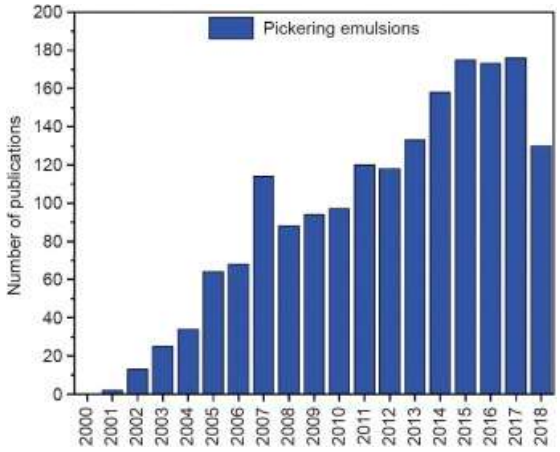


**Figure 3: Number of Pickering emulsions-related papers per year (2000–2018) [7]**

## 3. Physical-chemical properties of Pickering Emulsions

Interfacial tension, adsorption energy, and interaction parameters that allow immiscible liquids to coexist, as well as the contact angles that particles can generate with phases, all play a role in determining the physical and chemical properties of Pickering emulsion that are described in the following section.

### 3.1 Interfacial tension

The force required to separate two impermeable liquids is known as the interfacial tension. When two phases (liquid and gas) are separated by an interface, cohabitation is feasible. For example, the Gibbs free energy Fs associated with contact surface A between two phases is depicted mathematically as a change in the free energy F associated with a change dA of a surface among two components: [8].

$$FS = \frac{\delta F}{\delta A} A = \gamma_{int} \mathrm{A} \qquad (1)$$

Energy per area or force per unit length is represented in N/m and is a unit of energy. When two different media come into contact, the free energy F associated with each site dA on the surface might change. This is known as interfacial tension. Tangential tension is responsible for reducing the interfacial area. To put it another way, if two phases are separated by a barrier with a free energy Fs associated with forming a contact surface A between the two phases, they can exist at equilibrium [8]. A variety of techniques, such as capillary ascent, hanging or falling drops, can be used to quantify interfacial tension, as described in great length in an article by Le Neindre B. [9].

### 3.2 Contact Angle

Contact angle is a measure of wetting when particles adhere at an intersection between both the oil and water phases. For the particles to be anchored at the interface, they must be partially wetted. The wettability of these particles is determined by the angle at which they come into

contact with the liquid-liquid interface. The interfacial energy of the solid and the two liquids are used to calculate the contact angle using Young's law [10]:

$$Cos\,\theta = \frac{\gamma_{s/o} - \gamma_{s/w}}{\gamma_{o/w}} \qquad (2)$$

where θ is the oil-water-solid contact angle defined in the aqueous phase, $\gamma_{s/o}$ is the surface energy between the solid particle and oil, $\gamma_{o/w}$ is the surface energy between oil and water and $\gamma_{s/w}$ is the surface energy between solid particles and water.

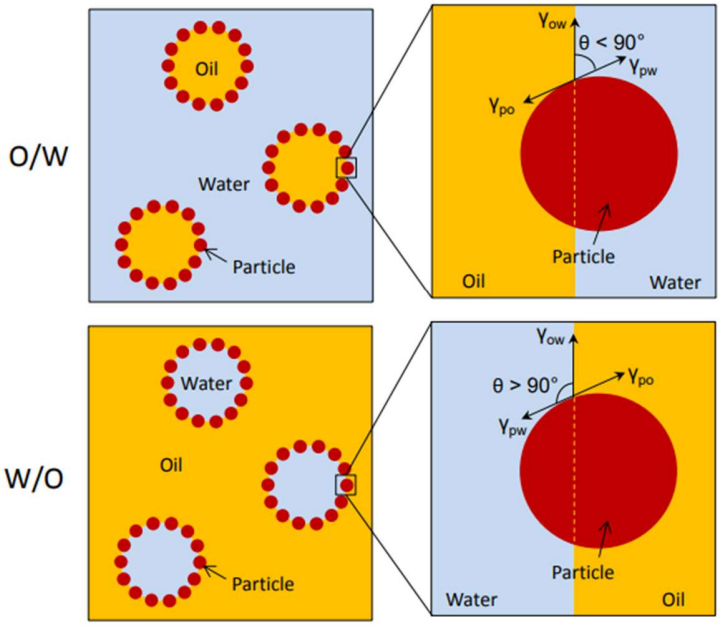


**Figure 4: Schematic representation of an oil-in-water and a water-in-oil emulsion at microscopic, and nanoscopic scales. The three-phase contact angle (θ) as well as the particle-oil ($\gamma_{so}$), particle-water ($\gamma_{sw}$) and oil-water ($\gamma_{ow}$) interfacial tensions are materialized on nanoscopic scale pictures (right) [51]**

The following empirical rule has been constructed for spherical particles considering the classical case of emulsions containing oil and water (illustrated in Figures 4). Particles having a contact angle above 90 degrees are hydrophobic, and the majority of the particle is in touch with the oil phase. Emulsions of the W/O (water-in-oil) emulsions type are obtained. When the contact angle is less than 90 degrees, the particles are hydrophilic and are mostly wetted by the water

phase. Thus, the emulsions are of type oil-in-water emulsions (O/W). This angle also corresponds to the particles' maximal energy at the contact.

To achieve the best stabilization of oil/water or water/oil emulsions, the contact angle must be close to 90° (measured on the water phase side) and the solid particles must be wetted by the external phase liquid more than the internal phase liquid [12]. In fact, Finkle et al (1923) [12] [13] and Binks and Horozov (2006) [14] demonstrated that stabilization is impossible if the particles are too wet by dispersed phase. Furthermore, Finkle established the following rule in 1923, linking the type of emulsion to particle wettability: that the phase that preferentially wets the particles will be the continuous phase of the Pickering emulsion. It is important to note that the medium in which the solid particles are introduced during the emulsion preparation also influences the emulsion's direction [15]. Indeed, because colloidal particles have a size and volume, the surrounding medium influences their mobility and adsorption at the interface. Binks and Lumsdon [16] demonstrated that if the particles are dispersible in both phases, the following behavior can be observed: the continuous phase of the emulsion is the one in which the particles are originally dispersed.

The contact angle of particles adsorbed at interfaces can be measured using a variety of methods. According to Destribats et al. [11] (and in the broad notions of his thesis [17]), there are numerous ways in the literature like FresCA, Cryofracture, interfacial cryofracture, and the gel trapping technique can be used.

### 3.3 Adsorption Energy

The high adsorption of solid particles at the liquid-liquid interface serves as a barrier against instability in Pickering emulsions. In order to remove the particle from the interface, this affects how much energy is necessary. The energy (-ΔadsG) necessary to remove a particle of radius r from an oil-water interface of interfacial tension $\gamma_{\text{oil-in-water}}$ is given by the following equation [18] [19].

$$-\Delta_{ads}G = \pi * r^2 * \gamma_{o/w} (1 \pm Cos\, \theta_{o/w}) \qquad (3)$$

The sign inside the brackets is negative when the particles are to be removed towards the aqueous phase, and positive for removing them towards the oil phase. The lower ($-\Delta_{ads}G$), the easier it is to remove the particles from the interface. Indeed, ($-\Delta_{ads}G$) depends on $r^2$, so this energy is low for small particles which could then potentially detach more easily from the interface [19]. A few orders of magnitude are however sufficed to understand the irreversibility of the particles at the interfaces, when the particles are small (of the order of ten nanometers).

Indeed, S. Arditty [20] demonstrates that the energy required to remove a particle from the contact is critical. Energy required to remove one particle from the oil/water interface is 1000kT if the particle's radius is 10 nm and its contact angle is 90° with the oil-water interface with an interfacial tension of 50 $mN.m^{-1}$ (kT corresponding to the thermal energy).

The order of magnitude of ($-\Delta_{ads}G$) is found to be between 0 and 20 kT in case for a surfactant. For example, for a non-ionic surfactant (Triton X-100) at a temperature T=25°C, ($-\Delta_{ads}G$) = 18.64kT [75]. This is because high energy results in a greater contact angle$15°>\theta>30°$**.** A particle up to 5 nm nanometers in diameter adsorbs permanently at the interface, while a surface-active molecule adsorbs and then desorbs reversibly at the same location. Small particles having a radius less than 0.5 nm (i.e., representative of the size of surfactants) have a lower adsorption energy than 10 kT, according to Binks B.P. [76]. Therefore, if the energy is so low, particles will no longer be able to stabilize the contact, as they will quickly desorb from it due to the angle in between $30°>\theta>15°$. Since working with such small particles can often exceed the detection limit for optical instruments (for example), it is extremely difficult to confirm this idea.

## 4. Interactions between Colloidal Particles in solution and at the interface

### 4.1 Interaction between Particles

The interactions taking place between two colloidal particles are responsible for most of the physicochemical properties of emulsions [48]. The interactions between colloids are strictly speaking the result of interactions between all the molecules present in the particles or the surrounding medium [22] [49]. On the one hand, attractive van der Waals in combination with

Brownian motion, are responsible for the flocculation of the particles. In contrast, repulsive interactions permit the formation of kinetically stable suspensions. This consists of charged colloids in aqueous phase. Electrostatic forces between the surfaces, which are shielded by the cloud of counter ions that gravitationally surrounds the surfaces, provide the repulsion. Derjaguin and Landau and then Verwey and Overbeek, within the framework of the DLVO model, estimated the exact potential of interaction between two colloids, taking into account van der Waals interactions and electrostatic repulsion forces [48]. As explained by McClement in his [48], the interactions are described in greater depth below:

### 4.1.1 Van der Waals Force

There are three distinct types of Van der Waals interactions to be aware of. All dipolar molecular interactions are included here:

1. Keesom interactions are between permanent dipoles are present. The configuration of the dipoles influences these interactions. There are polarities in the molecules.
2. Interactions between induced and permanently magnetized dipoles known as Debye interactions. The molecules are both polar and non-polar.
3. Induced electrostatic dipole interactions are known as London interactions. Molecules do not have any polarity.

Two colloidal particles' Van der Waals interaction range is only a few hundred nanometers. When the two particles come into touch, the interactions will be different from each other. If the two colloidal particles have different chemical properties, the interaction will be repelled, whereas if the two colloidal particles have equal chemical properties, the interaction will be attracted. Flocculation can occur whenever the Van der Waals forces are strong enough [20]

### 4.1.2 Electrostatic Stabilization

Charged particles can be used to stabilize colloidal suspensions. Aqueous is an illustration of a nonpolar media in which the opposing ions form an electronic dual layer with charged

surfaces, while in a polar medium, the opposing ions produce an electronic dual layer while the ion pairs likely to disintegrate. The entropic repulsion then displays itself. [48]

Electrostatic interactions are attracting when two colloidal particles have opposing charges, but repulsive when the charges match. This is important to remember (which is generally the case). When colloids move away, the strength of this contact is reduced and can be short- or long-range depending on the ionic strength and dielectric constant of the electrolyte solution surrounding them. Particle size has an effect on the strength of the interaction [48].

### 4.1.3 Steric Stabilization

These interactions are caused by interfacial entanglement or compression. Entropy is the source of their existence. A high steric interaction prevents colloidal particles from aggregating when they are near together. If the distance between the two colloids is small, this form of contact is strongly repulsive, but it can also be attracting or repulsive if the distance is intermediate (depending for example on the quality of the solvent present in the suspension medium of the particles). Steric interaction range and strength both increase with particle size as the adsorbed layer thickens [48]. Additionally, colloidal particles can be stopped from becoming aggregated by the addition of a polymer to their surface [20].

### 4.1.4 DLVO Theory

In this theory, the whole interaction capability between two colloidal particles is taken into account in this hypothesis. There is consideration given to both Van der Waals interactions and electrostatic interactions. Steric interactions, which have a very small radius of action, may also be implicated in this process. Derjaguin, Landau, Verwey, and Overbeek developed the term "DLVO theory" to describe the total of these interactions. It is this repulsion that forms an energy barrier that prevents colloidal particles from reaching a distance at which the attractive interactions are strongest. When this potential barrier is broken down, however, the particles have a greater chance of aggregating [48].

## 4.2 Interactions between Particles at the liquid/liquid interface

Pieranski P. suggested the dipole-dipole interactions [21]. After that, Hunter et al. explained in their article on emulsion stabilization that Pieranski P. was the first to express that dipole were generated via an asymmetric charge distribution of the particles [22]. Particles in the aqueous phase are ionized as a result [23]. [21]. Charge distribution on the surface of particles having ionizable groups (latexes or silicas) causes the emergence of dipoles parallel to the interface, which is caused by an uneven charge distribution on the particle. DLVO, the double ionic layer that surrounds the particles, is responsible for this dipole-dipole interaction. At the contact, the particles repel each other. When the particle is submerged in water, it has the ability to neutralize its own charge. The stronger the dipole-dipole interaction, the more hydrophobic the particles are, which makes sense [23].

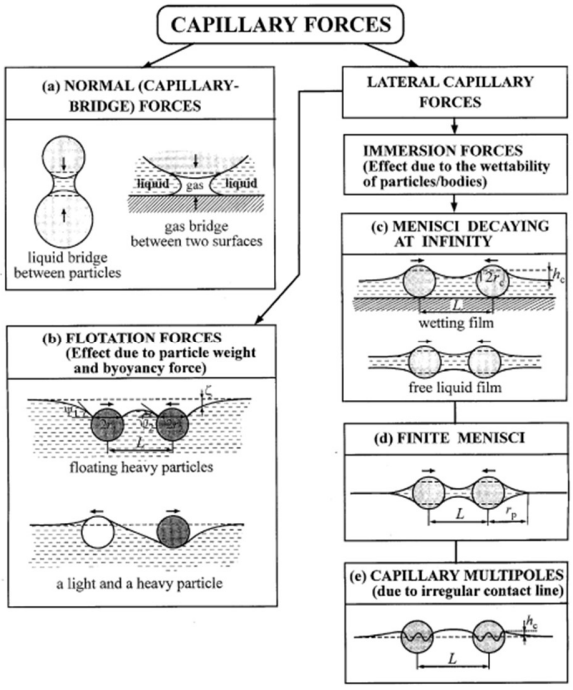


**Figure 5: Different types of capillary interactions [24]**

There are various types of capillary interactions, including gravitational interactions, wetting interactions, and interactions caused by irregularities in the contact line as mentioned in figure 5. In each of these instances, capillary interactions result from a deformation of the interface.

When particles are large or extremely dense, they deform the interface due to the force of gravity; the resulting attractive interactions are known as buoyancy. These forces become negligible for particles smaller than one micron because the particle weight is insufficient to deform the interface. Wetting deforms the interface if the particles are located on a solid substrate or in a thin liquid film. Immersion is then used to describe the associated attractive interactions, which persist even for particles with a radius smaller than one micron. In addition, the interface may be deformed if the contact line on the particle's surface has irregularities. This type of irregularity is the source of attractive interactions, which can be significantly greater than kBT, as described by Kralchevsky et al. [24]. Due to the difficulty in estimating the characteristic size of the line's irregularities, the energy linked with these capillary interactions can only be considered as part of order of magnitude. [24].

## 5. Destabilizations of Pickering Emulsions

The main mechanisms of destabilization of a Pickering emulsion can be separated into two categories irreversible (Ostwald ripening or coalescence).

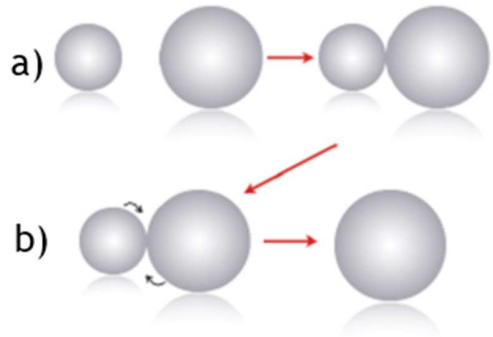


**Figure 6: Schematic Representation of a) Coalescence b) Ostwald Ripening [73]**

1. Ostwald ripening: It occurs when emulsions are aged over a long period of time. Due to pressure differences, molecules from the smallest droplet migrate up to the largest one. This process continues until all of the molecules have moved up to the largest possible droplet [25]. There is a tightening of the drop size distribution of emulsion droplets as a result. The dispersed phase must be somewhat soluble in the continuous phase for this

instability to occur. Small droplets and soluble dispersion phase make this self-regulating process much more apparent [25]. When the average drop diameter is bigger than 1 nm, ripening is extremely inactive [26].

2. Coalescence: The collapse of emulsions is also caused by coalescence, a second key mechanism. Coalescence occurs when two or more emulsion drops combine to produce a single drop that has a wider diameter than the initial diameter of each drop. This event is easy to identify since it can result in full emulsion separation as a result of drop fusion. In theory, the flocculation process, which allows droplets to become closer to one another, is always a precursor to the coalescence process. In fact, a merger of the two nearby interfaces is required. The thinning of the interfacial film, which eventually leads to its rupture, is the initial step in this integration. To counteract the coalescence effect in Pickering emulsions, colloidal particles deposited irreversibly on the surface of the drops create an electrical or a steric barrier. [17]

## 6. Limited Coalescence Mechanism of Pickering Emulsions

At the oil-water interface, solid particles are strongly and irreversibly adsorbed, resulting in the creation of a dense film that acts as a barrier to the drops and greatly increases their resistance to coalescence. It's possible that the droplet contact may at first be held in place by solid particles. Some of these particles have a completely naked interface. The droplets can agglomerate and combine in these regions. When two or more droplets combine, they grow in size. Coalescence halts when the interface is completely covered by the particles and there are no particles left, and there is no bare surface for the droplets to combine. Coalescence has halted. Droplet stability is achieved. "Limited coalescence" is the technical term for this mechanism (Figure 6). As a result of this phenomena, the emulsions themselves are very uniformly disseminated. First, Wiley documented the "limited coalescence" phenomena in Pickering emulsions in 1954 [28]. Limited coalescence requires two hypotheses: they are initially not enough particles to recover the total interfacial area, this means a particle poor-regime and once adsorbed, particle remain adsorbed (irreversible adsorption).[20]

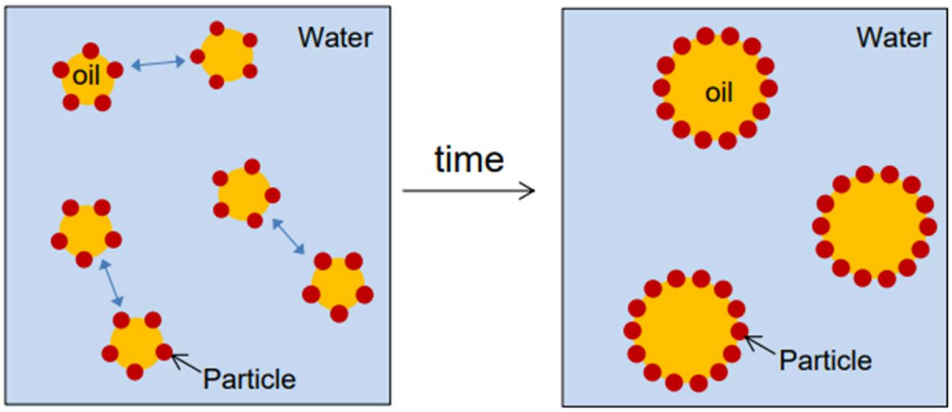


**Figure 7: Schematic Representation of Limited Coalescence. Double arrows show droplets approaching closer to each other. [51]**

An irreversible bond between solid particles and the liquid-liquid interface allows them to arrange in various ways. The particles can be used to protect the emulsion from instability by partially or totally covering the interface, or even in multilayers. The expression "coverage rate" is used to describe this. In simple geometrical considerations, the surface covered is given by when all particles are assumed to be adsorbed at the interface. [17]

$$C = \frac{m_p * D}{4 * \rho_d * d_p * V_d} \qquad (4)$$

where D the final diameter of the emulsion droplet, $m_p$ the particle mass, $\rho_d$ the particle density, $d_p$ particle diameter and $V_d$ volume of dispersed phase.

The percentage of the drop's interfacial area that is covered by the particles is referred to as the covered surface. Particles at the interface are said to be compact when this property is present. For a compact hexagonal stack, C, for example, is equal to 0.9. The stack is aerated if C is smaller than 0.9. In contrast, if C is more than 0.9, the particles is piled in multilayered structures or aggregates [17]. This parameter made it easier to comprehend the organization of the particles at the liquid-liquid interface provided below, followed by the presentation of the particles' existing interactions.

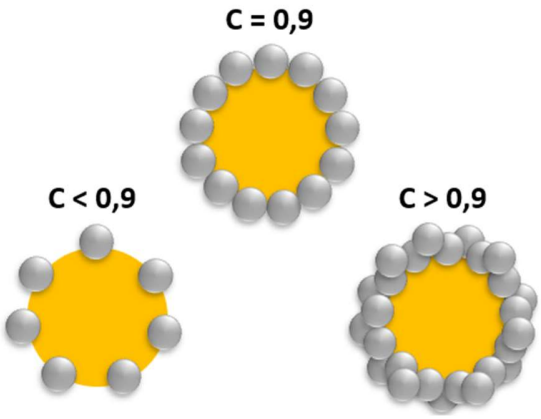


**Figure 8: Schematic Representation of Surface Coverage (C) in Pickering Emulsion**

## 7. Compression Behavior of Pickering Emulsions

Arditty et al. [20] were interested in the volume properties of Pickering emulsions stabilized by silica particles to deduce the mechanical properties of the particle-covered interfaces. For this purpose, the "osmotic" pressure of emulsions was measured by centrifugal tests for volume factions above the compact hexagonal stack ($\phi > 64\%$). Indeed, in the concentrated regime, the droplets on contact deform and the increase in their surface area is all the greater as the volume fraction is higher. By calculating the pressure ratio $\pi$ / $(\frac{\gamma}{R})$ which corresponds to the osmotic pressure normalized by the Laplace half-pressure; the authors found that this ratio is much greater than that obtained for emulsions stabilized by surfactants. They then deduce that the deformation of drops in emulsions stabilized by solid particles is not controlled by the Laplace pressure of the undeformed drops but by the ratio where $\pi$ is a parameter characterizing the rigidity of the drop surface. This can be justified by considering that the interfaces behave as two-dimensional solids due to the lateral interactions (capillary and hydrophobic) that can exist between neighboring particles. At low deformations, the interfaces have an elastic behavior and then they present a plastic behavior at intermediate deformations. The parameter $\pi$ corresponds to the surface stress threshold which marks the transition from an elastic to a plastic regime (two-dimensional flow threshold) [20].

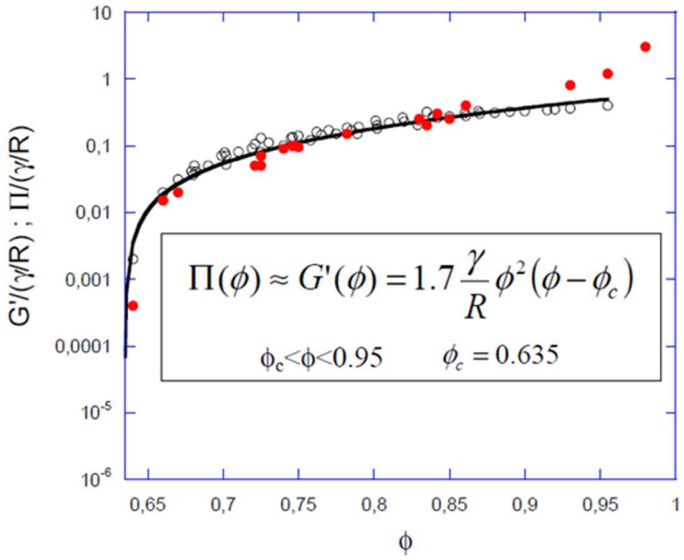


**Figure 9: obtained for concentrated monodisperse emulsions stabilized by surfactants [20]**

## 8. Thermoresponsive Polymers

Polymers that can alter their physical and chemical properties based on a specific temperature stimulus are known as thermoresponsive polymers. According to whether they have a lower (LCST) or an upper (UCST) critical solution temperature, thermoresponsive polymers can generally be divided into two groups [77] [78]. Polymers in both classes have varying physicochemical properties when heated to a specific temperature. Low temperatures render UCST polymers insoluble, but an enthalpic process causes them to dissolve above the UCST [79]. On the other hand, LCST-type polymers engage well with their solvents at low temperatures, but when heated above their LCST, they undergo a sharp coil-to-globule transition and leave the solution as entropy increases. Hydrophobic effect [80] of water is the root of both mechanisms and can be described as a binary system composed of the solvent (or a mixture) and the polymer, with their mixability dependent on temperature and polymer fraction. The binodal boundary is the temperature at which demixing occurs at each individual volume fraction of the polymer at which the phase boundary is defined [81]. Polymers with thermoresponsive properties have made significant contributions to biomedical applications over the past 50 years [77] [78].

## 8.1 Microgels

A type of particles known as "soft particles" has been extensively examined over the past two decades. These are polymeric colloidal particles with a size between 100 and 1000 nm that are weakly cross-linked and capable of swelling with a solvent [30]. Baker created the term microgel in 1949 [31]. The most prevalent microgels are thermosensitive microgels, which are derived from polymers whose solubility is temperature and dispersion phase-dependent. Indeed, microgels expand or shrink based on the temperature conditions and solvent quality.

Microgels can be generated via emulsion polymerization, precipitation or dispersion polymerization, crosslinking of self-assembled polymers, or in a restricted environment [32-37]. According to the scientific literature, dispersion polymerization is the most common synthetic method for generating heat-sensitive microgels. Pelton and Chibante established this synthesis process in 1986 under the term "Surfactant-Free Emulsion Polymerization" (SFEP) [37]. Monophasic at the outset, precipitation polymerization is a free radical dispersion polymerization process. In the continuous phase, the monomers, initiators, crosslinking agents, and stabilizers are soluble and dissolved. The monomer chains are initiated in the aqueous phase and form water-soluble oligomers until they reach a threshold size, at which point the expanding polymers become insoluble and precipitate as particles [37]. Figure 10 is a summary of the precipitation polymerization process processes. Poly(N-isopropylacrylamide) (pNIPAM) is the most studied synthetic thermoresponsive microgels. [40]

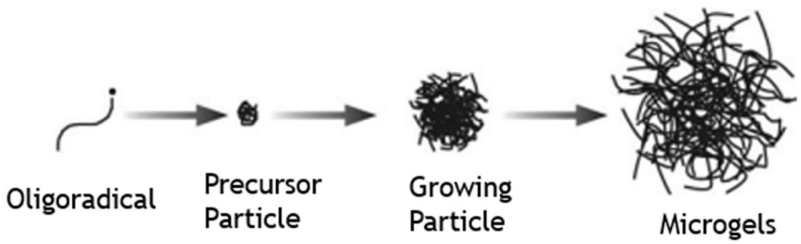


**Figure 10: Precipitation Polymerization [37]**

## 8.2 General Information about pNIPAM microgels

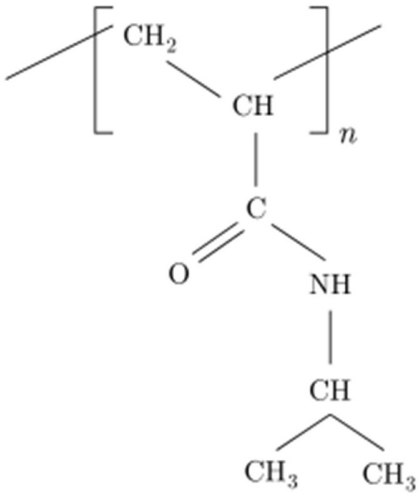


**Figure 11: Chemical Structure of pNIPAM**

Poly (NIPAM)-based microgels are the first examples of spherical and monodisperse particles synthesized by precipitation polymerization in aqueous medium in the absence of any surfactant. This method is based on the critical solubilization temperature (LCST) of polyNIPAM equal to 32°C and above which the polymer is no longer soluble in water. In this synthesis, NIPAM and the crosslinker, N, N'-methylene bisacrylamide (BIS) are dissolved in water and the mixture is heated to a temperature above the LCST of the polymer. Polymerization initiators are chosen to be water soluble and thermally decompose into radicals. They are usually potassium or ammonium persulfate or azo compounds. When the growing chains reach a critical length, they precipitate by adopting a globular conformation in spherical form under the effect of the temperature higher than the LCST of the polyNIPAM and form the precursors of the particles called nuclei. The nuclei will then continue to grow either by aggregating with each other or by adsorption of other oligo-radicals or by addition of monomers until they reach a stable particle size in the medium [37]. The spherical shape of the microgels is maintained when the temperature is lowered below the microgel volume phase transition temperature (VPTT) due to the cross-linking nodes formed by the cross-linker which prevents any redispersion of the polymer in solution. The colloidal stability of the particles

is ensured either by surface charges from the initiator (electrostatic repulsion) or by steric effect of the polymer chains in good solvent [38].

The number of charges present during synthesis can influence the eventual size of the microgels, which is governed by the surface charge density of the nuclei formed during precipitation. In fact, the bigger the surface-to-volume ratio, the smaller the particle size, the more stabilizers are needed. Smaller objects can be produced because surfactants, for example, allow the development of microgels to be stable sooner in the polymerization process [34, 38]. Researchers found that the diameter of poly (NIPAM) microgels could be lowered by a factor of up to 10 when SDS molecules were added before polymerization was started. To increase the surface charge of the nuclei, SDS molecules adsorb onto the growing polymer particles during the production process. As a result, aggregation of particles is prevented, increasing their colloidal stability. A smaller final diameter is achieved because the solution's concentration of forming particles rises (growth limitation). [38]

The original behavior of pNIPAM makes it a polymer studied for many applications. In optics, applications such as filtering and wavelength tuning are contemplated. The main field of application of the pNIPAM is that of the life sciences; the polymer is often conjugated to biological objects (antibodies, enzymes, etc.) to make them heat-sensitive; it is thus possible to carry out immunoassays using affinity precipitation based on a PNIPAM bioconjugate. PNIPAM is also used as a shell around solutes, for drug delivery applications. PNIPAM layers, hydrophobic at human body temperature, also serve as cell culture media and allow gentle release without enzymatic digestion [77] [78].

### 8.3 pNIPAM microgels in a Solution: Behavior and Properties

Polymer-polymer or polymer-solvent interactions show a major role in determining the conformation of pNIPAM in an aqueous solution. NIPAM is able to create hydrogen bonds with the solvent due to its amide functionalities because of its chemical structure. The laterally isopropyl groups, on the other hand, generate hydrophobic connections between molecules [39]. At 32°C, the transition temperature (LCST) for linear polymer chains in dilute water is between the solvated

and contracted states. At Low temperatures (32°C) enhance polymer-solvent interactions, and the polymers take on a statistical ball shape. A polymer-rich and polymer-poor phase can be detected when the temperature rises over the LCST, since the hydrogen bonds at the origin of polymer solvation are unfavorable and hydrophobic interactions take superiority. [39,40]

Same as for linear polymers, the conformation of the pNIPAM microgel is determined by the balance of osmotic pressures associated to chain swelling (Flory parameter) and the elasticity of the network, controlled by cross-linking density. VPTT (Volume Phase Transition Temperature) is somewhat above the LCST of the corresponding linear polymer when it comes to microgels. At lower temperatures, the microgels swell, with polymer-solvent interactions providing the most favorable conditions for enlargement. Dehydration of microgels occurs when the temperature rises above the VPTT, which causes them to compress (Figure 12). [39,40]

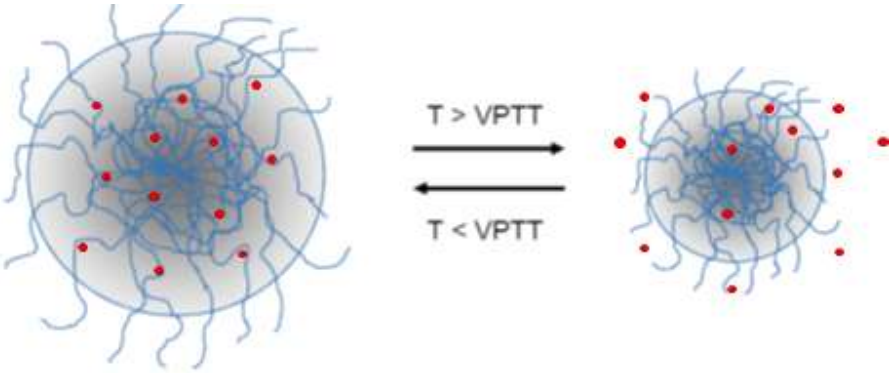


**Figure 12: Behavior of pNIPAM (before and after Volume Phase Transition Temperature {VPTT}) [52]**

## 8.4 Organization of pNIPAM at the oil/water interface

A study by Destribats et al. [17] attempted to demonstrate that the limited coalescence phenomena could also be used to deformable particles, such as microgels. This was accomplished by creating a variety of emulsions using various microgel amounts and cross-linking rates. A linear relationship between drop diameter and the number of microgels delivered into the aqueous phase was found in the particle-poor regime. Coverage rate C does not depend on cross-linking rate of

microgels because all curves can be superimposed (Figure 13). Moreover, this experimentally determined single coverage rate is just 40%, which is significantly lower than the 90% value expected for a compact 2D hexagonal arrangement of monodisperse hard spheres in a 2D hexagonal configuration. This indicates that the microgels are distributed on the surface of the drops in a hexagonal pattern with a mesh parameter that is significantly greater than their hydrodynamic diameter in solution. The authors then propose two hypotheses: either the oil/water interface is truly poorly covered and the microgels are structured in a non-compact fashion (no contact between them), or the adsorbed microgels can deform at the oil/water interface. [17].

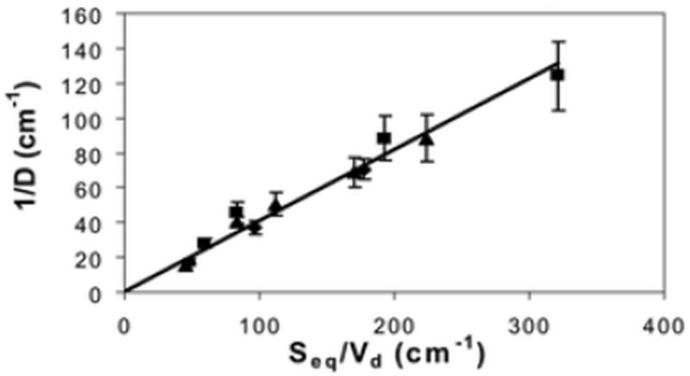


**Figure 13: Evolution of inverse of Diameter (1/D) as a function of Surface of equatorial region (Seq) normalized by Volume of dispersed phase ($V_d$) [17]**

## 8.5 Morphology of pNIPAM at oil/water interface

To determine the actual organization of microgels on the surface of drops, direct visualization of the interface is necessary, which has required the development of new imaging techniques. The first images of adsorbed microgels on the surface of emulsion drops were obtained by Ngai et al [41].

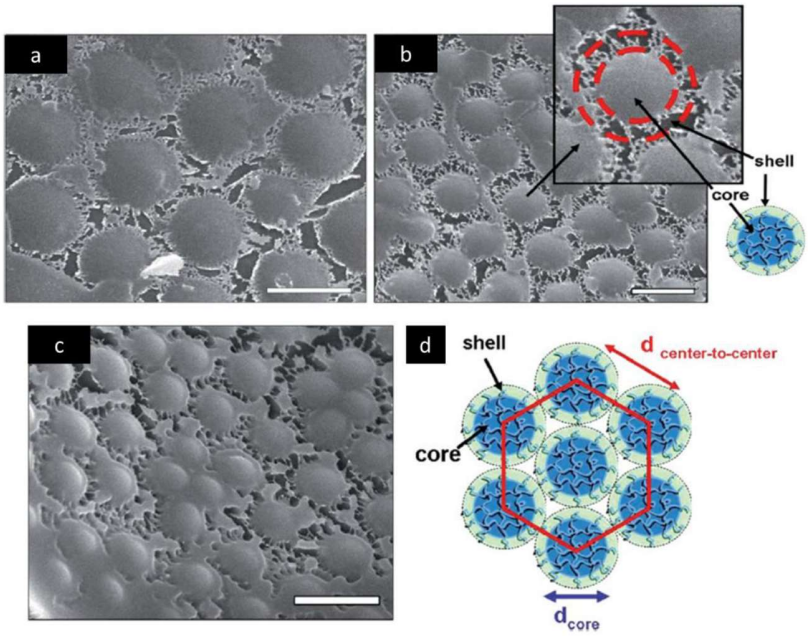


**Figure 14: Cryo-SEM image of the interface of a heptane-in-water emulsion drop covered by: a) and b) 2.5 mol% BIS cross-linked microgels after sublimation (front view), c) 5 mol% BIS cross-linked microgels after sublimation (sidelong view), scale bars are 1 mm; d) scheme of the particle structure and arrangement at the interface. [27]**

Later, Destribats et al [27] used confocal fluorescence microscopy and Cryo-SEM to examine how neutral pNIPAM microgels organize themselves on the surface of emulsion drops. Microgels can be seen on the surface of the drops using fluorescence microscopy, although this method is still limited since the distribution of fluorescent monomer within the microgels is not always uniform. As a result, Cryo-SEM conducted a thorough investigation to show that the microgels on the drops' surface deformed. The microgels appear to cover the interface in a regular hexagonal arrangement, with a highly cross-linked core in the center and a less cross-linked shell due to the inhomogeneous distribution of the cross-linker, as depicted schematically by the authors as deformable particles with a so-called "core-shell" structure (Figure 14). The fine structure of the microgels at the heptane/water interface can be disclosed following a sublimation process. The polymeric digitations (also known as pendant chains) of the shell deform, flatten, and connect the microgels, as seen by Brugger et al [50]. Using a "fried egg" structure (the "white"), the authors proposed a microgel model with an outwardly protruding "yellow" core that is more distorted due to its lack of cross-linking than the "white" shell used in the previous model (the "fried egg") (Figure 14 b). Because microgels are distorted at the water-oil interface, this theory is confirmed.

## 9. Analysis of the origin of the Flocculation of Pickering Emulsions

The macroscopic view of Pickering emulsions stabilized by pNIPAM microgels demonstrates that the emulsions were flocculated. This is demonstrated by the fact that the drops are aggregated and form, after creaming, a rigid block that adopts the shape of the container and does not flow out when the container is inverted, as shown in the Figure 15 a).

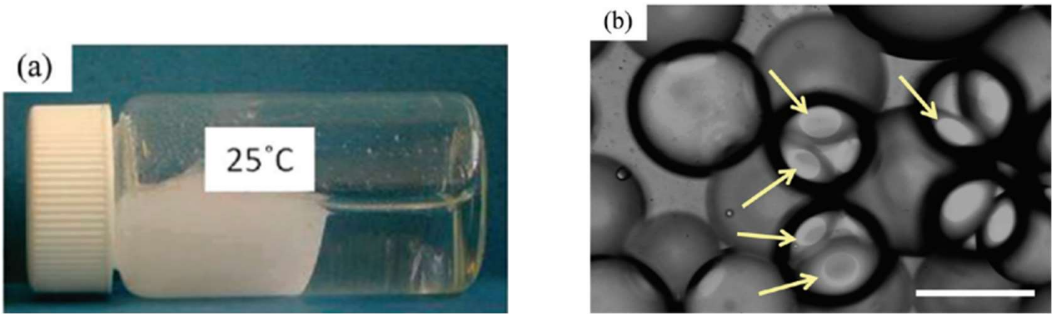


**Figure 15. a) Macroscopic image of a dodecane-in-water emulsion stabilized by 3.5 mol % BIS cross-linked microgels, b) Optical microscopy image of a hexadecane-in-water emulsion stabilized by 1.5 mol % BIS cross-linked microgels. The scale bar is 200 µm. The arrows indicate the presence of adhesive films in between two drops [43]**

Destribats et al. wanted to investigate the nature of where this flocculation came from [43]. A preliminary examination of the drops carried out using optical microscopy revealed that the drops have been distorted and that they are forming an adhesive coating between one another (Figure 15 b). The scientists were able to deduce an angle of adhesion between the two droplets by viewing the ellipse generated by this adhesion between the two drops. This angle of adhesion could also be calculated by a profile view of the droplet surface obtained using Cryo-SEM (Figure 16a).

The capability of the microgels to bridge the interfaces between two neighboring drops was brought to light by a detailed examination of the structure of the adhesive films carried out by Cryo-SEM. On the surface of the flat films, this causes the production of digitations and constriction lines, which are areas of thinner thickness that separate the digitations (Figure 16 b). After the films have been completely sublimated, the polymeric skeleton of the film can be seen: the contact areas between drops are made up of two interfaces, each of which is covered by a layer of microgels (Figure 16 c). In addition, the adhesion between two neighboring drops is of even

greater significance as the quantity of microgels bridging the gap between the two drops increases. [43]

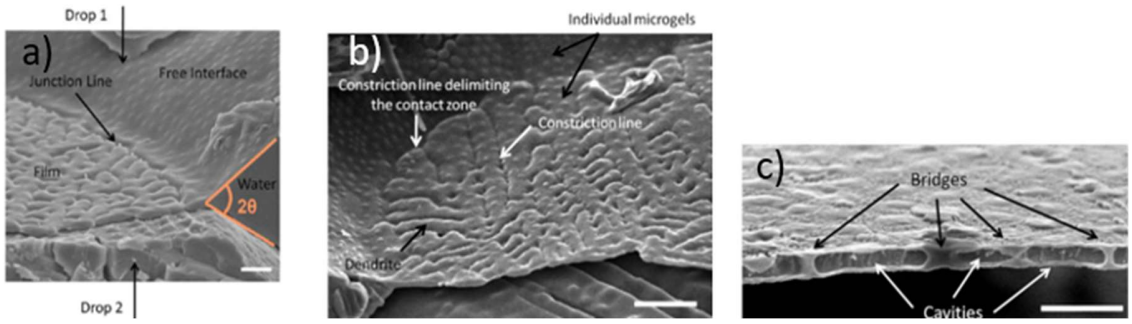


**Figure 16: a) Cryo-SEM image of an adhesive film between two dodecane drops stabilized by 2.5 mol % BIS microgels. Scale bar is 2 µm. b) . Cryo-SEM image of an adhesive film between two dodecane drops stabilized by 3.5 mol % BIS microgels. Scale bar is 5 µm. c) Edge views of fully dehydrated films between heptane drops stabilized by 2.5 mol % BIS microgels. Scale bars are 1 µm [43].**

## 9.1 Influence of Cross-Linking Density

It was determined that just one structural parameter, such as the cross-linking rate, could affect the qualities of the emulsions produced. The influence of cross-linking and, consequently, deformability on the same size microgels has been examined. Microgel cross-linking improves connection density, which is important for flocculation, as the rate of cross-linking increases. Microgels' deformability has also been proven to have a significant impact on the stability and mechanical strength of emulsions at rest. As the degree of cross-linking decreases, so the degree of interfacial deformation decreases than this results in improved compressibility and an improved ability to organize themselves tightly on an interfacial surface. A dense and elastic 2D interconnected network is formed when the cross-linking density is low. This network effectively protects the drops from flocculation. Ultimately, the stabilization efficiency is higher when the deformability is higher and the cross-linking density is decreased. Finally, it can be concluded that microgels with the lowest crosslinking density offer the best resistance to coalescence and the lowest probability of bridging flocculation. The droplets of highly cross-linked microgels are unable to stabilize because they slow the unfolding dynamics required for segment adsorption, and as a result they strongly flocculate. Different cross-linking rates of microgels were used in the formulation of emulsions. Emulsions made with microgels that are highly cross-linked (5 % BIS) are fragile, and all it takes to create a phase separation between water and oil is a simple mechanical

stimulation. At room temperature, however, the low-crosslinker formulation of microgels (1 % and 2.5%) is stable for several months. Microgel contraction can be used to test the impact of cross-linking on emulsion stability. [27]

### 9.2 Influence of Microgel's Size

Pickering emulsion stability and characteristics are also affected by the microgel size. Pickering emulsions can also be stabilized with smaller microgels (diameter of roughly 250 nm), as demonstrated by Destribats et al [43]. They flattened and distorted like a "fried egg" at the interfaces, just like the bigger microgels. A more densely covered interface was found to have lower deformability and spread ability at interfaces when smaller microgels were compared to bigger ones using coverage ratio measurements. Emulsions produced as a result of this process have weaker flocculation and are therefore more easily driven (Figure 17). A change in the structure of microgels is to blame for this poorer spreading capacity. Researchers Andersson et al. [44] and Arleth et al. [45] have proven, in fact, that the smaller microgels' lesser deformability is related to the synthesis circumstances' more homogenous radial cross-linking density.

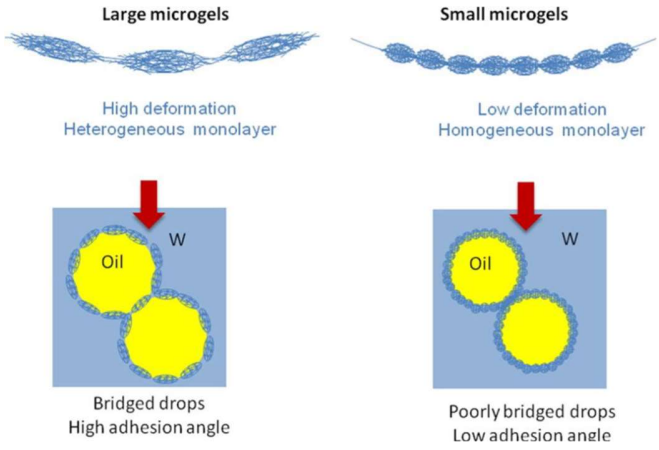


**Figure 17: Dependency of size of microgels on arrangement at oil/water interface [43]**

Polymer density profiles derived from these studies can be summarized using an effective polymer density profile that combines coverage rate C and interpenetration of pendant chains forming the shell. Bridging between adjacent drops is less desirable when the polymer monolayer is dense and homogenous (in a compact arrangement). For small or low cross-linking rate

microgels, the interpenetrations of the shell's peripheral chains enable fast adsorption at the interface and subsequent rearrangement. Microgels with less of a shell and less interpenetration of their chains, such as stiff (more cross-linked) or big ones, do not cover the interface as uniformly as shown in above figure 17. Contact zones between the drop interfaces are more likely to form in this configuration, which aids in the bridging and flocculation of emulsions. [46]

### 9.3 Influence of Emulsification Processes

Emulsions' flocculation properties can be adjusted using the emulsification energy. Strong shear deforms and flattens microgels, but low shear resulting in a heavily coated interface with microgels that are laterally compressed and so have the potential to overlap, as the researchers discovered using droplet surface measurements (Figure 18). Previously, emulsions had been bridging between neighboring drops. Destribats et al. suggested a conflict between microgel adhesion, relaxation mechanisms, polymer segment adsorption and recombination to describe how microgel organization happens at interfaces. Low shear rates produce dense monolayers in which the microgels are laterally compressed, whereas high shear rates result in the microgels being strongly flattened. As a result, the resulting emulsions exhibit contradictory flocculation behavior, which is caused by bridging between neighboring drops and is highly dependent on their surface coverage. Using a high emulsification energy to create a large volume of interface results in a lower surface density which results surface coverage less than 90%. Chain extension causes significant distortion of the microgels at the point of contact. A lesser volume of interface is generated at lower emulsification energies because of this. Microgels with a more compressed shape can be applied to the droplets' surfaces with longer exposure times, giving the impression that more was added than was actually needed to the solution. The pendant chains of the shell could be employed to join the microgels laterally in order to attain a higher density and more stable emulsions. [47]

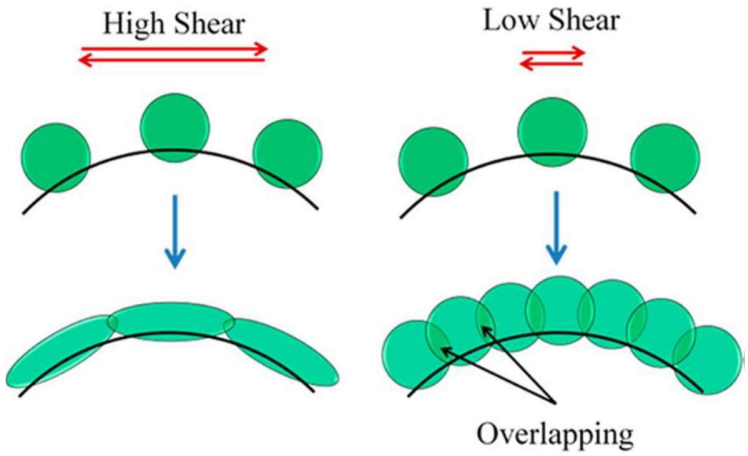


**Figure 18: Dependency of shear energy on arrangement of microgels at oil/water interface [47]**

### 9.4 Influence of Nature of oil

Depending on the kind of oil phase, the oil–water interface's interfacial tension and particle interactions are both affected. The viscosity parameter is also significant in the oil phase of the system. A silicone oil emulsion stabilized by glass beads was examined by Tsabet and Fradette [52] in which the salinity and pH of the aqueous phase were regulated. They discovered two distinct regimes of drop diameter as a function of the oil's viscosity.

1. Until a certain viscosity value is reached, the diameter of the drops remains constant. Coverage potential determines how quickly a system can stabilize once a large decline has occurred.
2. Drop diameter increases significantly when the viscosity is increased, as the entire emulsion process is affected.

As a result, the droplets' surface mobility is reduced, making it more difficult for the particles to adhere to them. In addition, the polarity of the oils is also a factor to keep in mind. Using hydrocarbons as a non-polar oil, Binks and Lumsdon [15] found that Pickering emulsions stabilized with silicas of intermediate hydrophobicity were more likely to form oil-in-water type emulsions. Emulsions of oils with polar characteristics, such as esters or alcohols, tend to be oil-in-water. In addition, they found that polar oils had a stronger effect on the oil-water contact than

non-polar oils did. In order for the oil molecules to tolerate the aqueous environment, their polarity must be large enough. To find a link between emulsion type stabilized using microgels and an oil polarity-related physical characteristic, this study looked for a correlation. The relative dielectric constant can be used to estimate the polarity of a solvent. As seen in figure 19, when it comes to dielectric constants, octanone and octanol share a dielectric constant of 10.4 and 10.3, correspondingly, however their emulsions have different curvatures. Due to which, the type of emulsion and oil's protic or aprotic nature are linked. As it turns out, the pNIPAM microgels are capable of stabilizing oil-in-water that include oils, such as alkanes. Knowing that these oils are susceptible to hydrogen bonding, that certainly promotes their contact to pNIPAM segments and furthermore their integration into microgels, such a relationship can be readily explained [54].

| oil type | emulsion type | ε |
|---|---|---|
| alkanes (heptane to hexadecane) | O/W | 1.92–2 |
| ketones (2-octanone and 5-nonanone) | O/W | 10.3 |
| aromatic hydrocarbon (toluene) | O/W | 2.4 |
| halogenated oil (bromocyclohexane) | O/W | 7.9 |
| halogenated oil (dichlorobenzene) | phase separation | 9.9 |
| silicone oil (PDMS 20 mP s) | O/W | 2.3–2.8 |
| fatty alcohols (1-hexanol to 1-decanol) | W/O | 8.1–13 |
| fatty alcohol (1-undecanol) | phase separation | 8.0 |

**Figure 19: Emulsion Type and Relative Dielectric Constant (in case of microgels) as a Function of the Oil's Nature [54]**

Based on the findings of this bibliographic research, it would appear that Pickering emulsions that are stabilized by stimulable and deformable microgels have been the subject of renewed interest during the past twenty years. The ability of these emulsions to be stabilized and destabilized on demand under the influence of one or more stimuli such as pH, temperature, light, and so on has been demonstrated by a number of groups as having potential in a wide variety of application areas. This ability has allowed these emulsions to be utilized successfully in a variety of contexts. The results that have been obtained on thermosensitive pNIPAM microgels have been the most fundamental and successful thus far. Numerous studies have been conducted to

investigate their structures according to the synthesis processes, their deformability, their arrangement and conformation at model interfaces or at the surface of emulsion drops, and so on.

Despite the fact that the Pickering emulsions have been the subject of extensive research and have been well documented ever since their discovery more than a century ago, it is still of utmost importance to investigate the stabilizing mechanism and interface properties in great detail for the purpose of application in a variety of fields. To the best of knowledge, the mechanisms that determine the stability of emulsions stabilized by these microgels are not completely understood at this time. In particular, it has been observed but not quantified that some microgel-stabilized emulsions are more resistant to mechanical disturbances than other [20]. This thesis is a component of a more conceptual approach that seeks to better understand the mechanical properties of microgel-stabilized emulsion interfaces. To do so, the approach is to study the compression behavior of these emulsions, which gives information about how interfaces respond when they are stretched. A particular point is to draw links between the structure of the microgels, the formulation processes, the manner in which the microgels adsorb and organize themselves at an interface, and the properties of the emulsions that are produced as a result of these processes.

# II Materials & Methods

## 1. Chemicals Used

Compounds from Sigma Aldrich were utilized in all experiments. A variety of chemicals, such as N-isopropylacrylamide (NIPAM) (quality >97%), Dodecane (quality >99.9%), N, N'-methylenebisacrylamide (BIS) (quality >99%), Potassium persulphate (KPS) (quality >98%), sodium dodecyl sulphate (SDS) (quality >98.5%), and polydimethylsiloxane (PDMS of viscosity 10 mPa.s), were employed without further purification. For the synthesis, emulsion preparation, and all other characterization procedures, Milli-Q water was employed.

## 2. Synthesis of pNIPAM microgels

In order to demonstrate the impact of the microgels' ability to deform, synthetic microgels, several batches of pNIPAM microgels were generated by radical polymerization by precipitation in an aqueous media in order to examine the effect of crosslinking and size on the morphological and mechanical properties of emulsions. The deformability of these microgels can be altered by altering the rate at which BIS is cross-linked, i.e., the initial mixture's BIS concentration (1% and 2.5%). Different set of microgels are prepared by adding or not surfactant (0- or 4-mM sodium dodecyl sulphate) to the monomer mixture to adjust the size of the microgels for (2.5 % and 5% BIS), just like the monomer mixture.

The analyzed microgels were synthesized by free radical dispersion polymerization in aqueous medium, which is a conventional approach for the manufacture of pNIPAM microgels. This polymerization was conducted in a 500 mL three neck round-bottom flask with a magnet bead, thermometer, argon inlet, and reflux column. N-isopropylacrylamide (NIPAM) was recrystallized in hexane and dried under vacuum before to use. The NIPAM and N, N'-methylenebisacrylamide (BIS), which acts as a crosslinker, were dissolved in 280 mL of water beforehand so that the total monomer concentration is 70 mM and remained constant throughout all syntheses. The crosslinker concentration varied 1 mol to 5 mol relative to the amount of NIPAM

in the combination. The mixture was heated to 70°C, under argon bubbling, for one hour. An aqueous solution containing 2.5 mM potassium persulphate (KPS) diluted in 20 mL water and cold degassed for 10 minutes under argon was added to start the reaction. The initially translucent solution becomes opaque, indicating that polymerization and precipitation have commenced. The polymerization continued for six hours at 70°C with stirring and argon bubbling. These set of microgels are termed as Large microgels in this thesis.

In the case of small microgels, the whole process is same except a surfactant, sodium dodecyl sulphate (SDS) with molar concentration (4 mM) was added to the NIPAM/BIS mixture. The molar concentration of crosslinker varies between 2.5 mol and 5 mol compared to the amount of NIPAM in the mixture. These are called as small microgels in this thesis. The chemical reaction involves to obtain microgels of controlled size and more or less cross-linked is mentioned in figure 20.

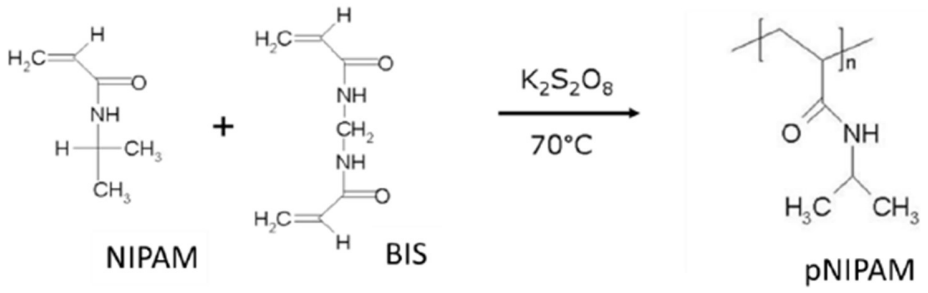


**Figure 20: Chemical Reaction Involved**

## 3. Purification of pNIPAM Microgels

To eliminate possible synthesis leftovers, such as water-soluble linear polymers, the microgels were washed seven times in clean water using centrifugation-redispersion (16,000 rpm or 29,000 g for large microgels for one hour per cycle). After each cycle of centrifugation, a phase separation is noticed between a more or less white, uniform deposit containing microgels as well as a clear liquid phase called supernatant. And the supernatants are gradually replaced by pure water. Using the pendant drop method, the surface tension of the final supernatant is then

determined. The final supernatant has the same surface tension as pure water (about 72 mN/m), indicating that the microgels have been entirely purified.

The small microgels could not be centrifuged because of their small size and low-density difference with water (solvent-swollen polymer). Therefore, these microgels were only purified by multiple cycles of dialysis utilizing a dialysis membrane (MWCO 100 kDa). In this procedure, the microgels were placed in membrane-prepared packages and properly sealed with clips. In the next step, the packets are placed in a beaker containing water and magnet beads and stirred at 400 rpm for seven days at room temperature. However, the water in these beakers is replaced twice day in order to obtain purified microgels. Then purified microgels were analyzed by DLS (Dynamic Light Scattering) in order to check their thermosensible behavior.

## 4. Microgels dispersion characterization

To determine the mass of polymer ($m_{pol}$) in a given dispersion, the dry extract method is used after the purification process (either centrifugation or dialysis). Then, weight, an aluminum cup is filled with around 1 ml of dispersion known as $m_{disp.}$ For 24 hours, this dish is dried at 50°C. It is thus possible to calculate the mass %age of microgels in the dispersion, also known as the dry extract (in % m) as follows:

$$\text{Dry Extract} = \frac{m_{gel\ (50\ °C)}}{m_{disp}} * 100 \quad (5)$$

Where $m_{gel}$ (50 °C) is the mass of microgels remaining in the cup after passing through the oven and evaporating the water in the solution.

It is therefore important to know exactly how many particles are in the suspension and deposited at the interface. As the microgels are swollen with water, it was considered that each particle is 71% wt of the polymer network and 29% wt of water at 50°C. It is therefore possible to number of particles in dispersion according to the formula of Lele et al [27], i.e.

$$n = \frac{6c_{polymer}}{\pi(d_{50°C})^3}\left(\frac{1}{\rho_{polymer}} + \frac{0.29}{0.71\rho_{water}}\right) \quad (6)$$

where $\rho_{polymer}$ is density of polymer i.e., 1.269 g.cm$^{-3}$ $\rho_{water}$ is density of water i.e., 1 g.cm$^{-3}$, $c_{polymer}$ is concentration of polymer, $d_{50°C}$ is hydrodynamic diameter of microgels calculated by DLS (Dynamic Light Scattering) and $\pi$ is 3.14.

## 5. Emulsions Production and Determination of droplet diameter

Emulsification is done by rotor stator homogenization (that is explained in more details in Annex-2) using large axis with rotor (18 mm diameter) and stator (25 mm diameter) or small axis with rotor (7.5 mm diameter) and stator (10 mm diameter). In case of large axis, the emulsions consist of 14 g of aqueous phase containing microgels (the amount microgels added was calculated by using microgel's concentration in dispersion) and 6 g of oil phase, which is typically dodecane (density $\rho_{dodecane}$=0.75g.cm$^{-3}$) or PDMS (density $\rho_{PDMS}$=0.93 g.cm$^{-3}$). In the case of a small axis, the emulsions consist of 7 g of aqueous phase containing microgels and 3 g of oil phase, which is most commonly dodecane or PDMS. The initial oil weight fraction $\phi_i^{wt}$ defined as the mass fraction of oil in the total sample is equal to 0.3. This phase separated mixture was then rapidly stirred for 30 seconds at a constant speed of 9500 rpm by an UltraTurraxT25 irrespective of the axis used. The emulsion is drawn into the gap between the rotor and stator by the axial movement generated by the rotor. The recombination/coalescence phenomenon is caused by highly energy collisions that occur as a result of the droplets fragmenting in the turbulent flow. As a result of this combination of fragmentation and recombination and limited coalescence, the drop size distribution is uniformly distributed. Emulsions are formed with a cream and a transparent aqueous phase, which indicates that all of the microgels are adsorbing at the interface and not remaining in the subphase. Figure 21 shows that emulsions created by this method are commonly flocculated [47] i.e., composed of drops that adhere to one another. The emulsion was allowed to rest overnight before to usage, allowing the relaxation and to stabilize the emulsion prior to analysis. The following concentrations of microgels are used for a limited coalescence curve: 0.005, 0.01, 0.015, 0.02, 0.03, 0.04, 0.05 %wt. The study of limited coalescence is discussed in detail in Results part of this thesis.

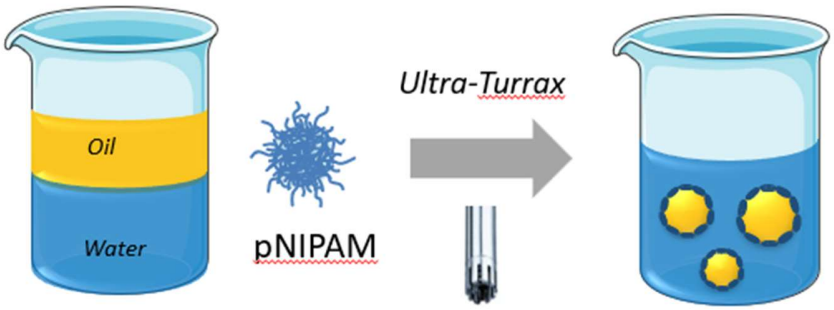


**Figure 21: Schematic Representation of preparation of Pickering Emulsions**

Optical microscopy is used to study the behavior of dispersed phase drops in the emulsion in order to quantitatively and qualitatively characterize the formed systems. Transferring the emulsion was done for optical microscopy of emulsions with the help of a plastic pipette (ideally 3 mL size pipet with a diameter larger than 3 mm). It must be ensured that emulsion is not disrupted by the pipet. When the transfer has been completed, do not cover the glass slide with a glass cover in order to avoid breaking. Images of the drop size distribution should be taken and analyzed (at least 50 drops).

It is possible to observe microscopic properties of a sample using optical microscopy. Coalescence and flocculation in Pickering emulsions can be studied using this method because it provides information about the drops' size and shape, allowing researchers to assess the stage of aggregation and flocculation. Static light scattering methods such as laser particle sizing were unable to detect the size distribution of the emulsions in this investigation because of the presence of adhesive drops in these systems. As a consequence, optical microscopy was used to extract the size distributions of these systems. The magnification used was x10. The images were recorded with a camera and the diameter of 50 drops was measured for each emulsion via ImageJ in order to establish a significant average.

Following the work of Destribats et al [27], the average drop diameter, also known as Sauter diameter, of emulsion droplets, indicated $D_{[3,2]}$ and the Polydispersity Index, PDI, defined was calculated by using equation 7:

$$D_{[3,2]} = \frac{\sum_i Ni\, di^3}{\sum_i Ni\, di^2}, \quad PDI = \frac{1}{\overline{D_m}} \frac{\sum_i N_i D_i^3 \, |D_m - D_i|}{\sum_i Ni\, di^3} \quad (7)$$

where $N_i$ is the number of drops of diameter $d_i$, $D_m$ is the median diameter, i.e., the diameter for which the cumulative undersized volume fraction is equal to 50%

## 6. Method for Compression

When it comes to the elastic properties of Pickering emulsion interfaces, compression is critical. Centrifugation was used to compress emulsions in this experiment, as shown in figure 22. A tabletop centrifuge (Allegra-X-22R Centrifuge) and 10 ml and 20 ml centrifuge tubes were employed in this experiment. Due to large drops sizes and density mismatch drops cream. The final oil volume fraction in the cream is given by

$$\phi_f^{vol} = \frac{\text{volume of oil}}{\text{volume of cream}} = \frac{\text{volume of oil}}{\text{total volume}} x \frac{\text{total volume}}{\text{volume of cream}} \quad (8)$$

As the oil volume is preserved, it can also be written as:

$$\phi_f^{vol} = \phi_i^{vol} x \frac{\text{total volume}}{\text{volume of cream}} \quad (9)$$

Where $\phi_i^{vol}$ is the initial oil volume fraction and is known from the composition and oil density It is linked to the oil weight fraction $\phi_i^{wt}$through:

$$\phi_i^{vol} = \frac{\phi_i^{wt}}{\phi_i^{wt} + (1 - \phi_i^{wt})\rho_{oil}} \quad (10)$$

In the case of PDMS, as the oil density is close to 1, it reduces to $\phi_i^{vol} \approx \phi_i^{wt}$ so that

$$\phi_f^{vol} \approx 0.3 x \frac{\text{total volume}}{\text{volume of cream}} \quad (11)$$

This approximation is no longer valid for dodecane due to the low oil density. Non interacting drops cream to reach the random close packing $\phi_{rcp} = 0.635$. A pressure has to be applied concentrate further the emulsion. The drops then deform. It is only the features of the interface that determine how much energy must be provided to the system to bring it to a volume fraction bigger than $\phi_{rcp}$ from this critical condition. Osmotic pressure in an emulsion is determined by the elastic characteristics of the interface at a specific volume fraction. The osmotic pressure of an emulsion is well-defined as the derivative of the total droplet free energy F with respect to the total volume V, at fixed dispersed phase volume $V_0$: $\pi = -\frac{\partial_F}{\partial_V}\Big|_{V_0}$ .For the compact stack, the osmotic pressure represents the energy required to stretch the surfaces by compression of the drops for $\phi_f^{vol} > \phi_{rcp}$.[20]

When the emulsion continues to be compressed once the compact stack is reached, the drops continue to deform until they break, characterized by the limiting osmotic pressure. $\pi^*$ It is possible to determine this osmotic pressure experimentally. Before breaking, π can be expressed as a function of $\phi_f^{vol}$, thus is defined the equation of state of a concentrated emulsion. The drops are initially spherical, so the interface between the two media is curved which results in a pressure difference $P1 - P2 = \frac{2\gamma}{R}$, called the Laplace pressure. The limiting osmotic pressure is thus normalized by the Laplace half-pressure $\frac{\gamma}{R}$ .

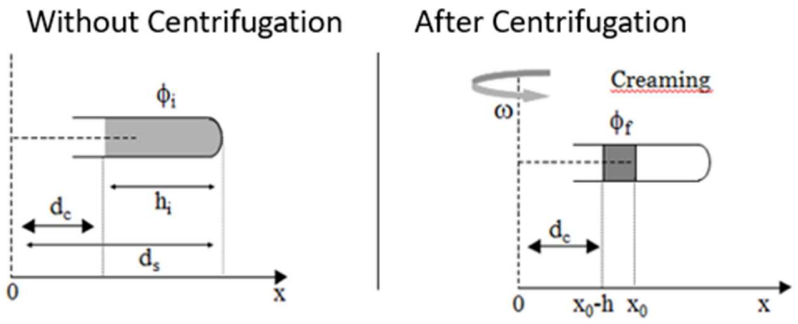


**Figure 22: Scheme for method of Compression**

In fact, the volume fraction is not constant in the cream, there is a gradient. However, the cream height is small (< 2cm) in front of the lever arm dc (9 cm) of the centrifuge, the volume fraction in cream is considered as constant and equal to $\phi_f^{vol}$. The osmotic pressure at the surface of the cream can therefore be expressed according to equation (12)

$$\pi_{max} = |\Delta\rho| * \phi_f^{vol} * \omega^2 * \left(d_c * h + \frac{h^2}{2}\right) \quad (12)$$

$|\Delta\rho|$ is the density difference between the continuous phase (water) and the dispersed phase. $\phi_f^{vol}$ is determined through equation (11) h represents the cream height after compression, it was measured by ruler after centrifugation and $\omega$ represents the centrifugation speed expressed in rad/s [20]. It is equal to: $\omega = 2\pi N/60$ where N is the centrifuge speed expressed in rpm.

It was necessary that the centrifugation time was done long enough for the stationary state to be reached. These states were accomplished in different emulsions by assessing the height of the cream of emulsions after each cycle (30 minutes each) of centrifugation at a given speed until it reached a constant value without emulsion breakage. The figure 23 below illustrates the method of determining steady state by showing the height of the cream as it varies over time.

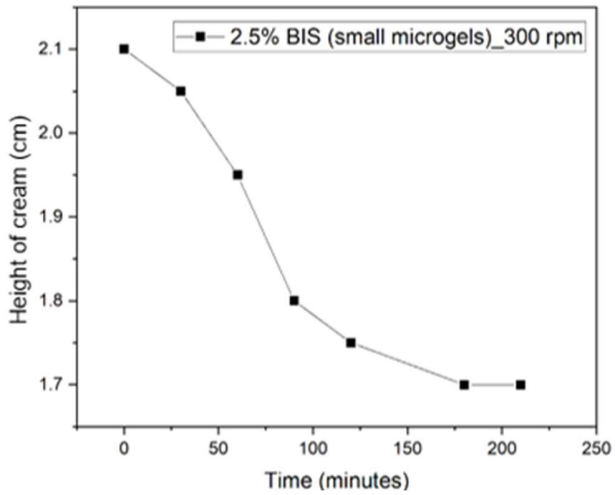


**Figure 23: Determination of steady state (in case of emulsions prepared by 2.5% BIS-small microgels with conc. 0.02% at speed of 300 rpm**

# 7. Characterizations Used

## 7.1 Dynamic Light Scattering

The Brownian motion of scattering particles is the basis for dynamic light scattering (DLS). Any direction can be reached once particles are spread throughout the liquid. Particles and solvent molecules constantly come into contact with each other in Brownian motion. The movement of particles is induced by the transfer of energy that occurs during these collisions. Smaller particles are more sensitive to the energy transfer so that the smaller particles are travelling faster. The speed sensitivity to particle size is therefore used to determine the hydrodynamic diameter in the absence of any other particle movement (sedimentation, convection due thermal gradient for example).[55]

The Stokes-Einstein equation describes the relationship between particle speed and particle size (equation 7). The translational diffusion coefficient (D) is used to determine the speed of the particles. Particle movement is directly influenced by temperature and viscosity; hence these two variables are included in the equation. The Stokes-Einstein equation requires that the movement of particles is purely Brownian motion. Because creaming or sedimentation can superimpose to the Brownian Motion DLS is adapted to the determination of particle size up to 1 or 2 µm. The figure 24 demonstrates about the working principle of DLS.

$$R_h = \frac{k_B T}{6\pi\eta D} \qquad (13)$$

Where $R_h$ = Hydrodynamic Radius (m)

D = Translational diffusion coefficient ($m^2/s$) – "speed of the particles"

$k_B$ = Boltzmann constant ($m^2kg/Ks^2$)

T = Temperature (K)

η = Viscosity (Pa. s)

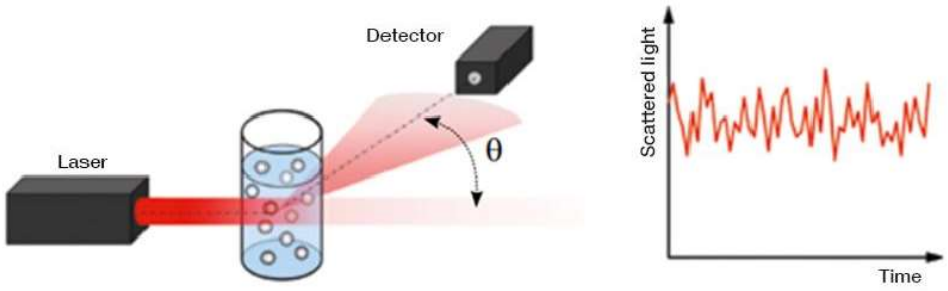


**Figure 24: Working Principle of Dynamic Light Scattering [55]**

Figure 24 depicts the basic configuration of a DLS device. A cuvette-contained sample is illuminated by a laser of a single frequency. If the sample contains particles, the incoming laser light is scattered in all directions. Using the Stokes-Einstein equation, the scattered light is measured at a specific angle over time, and this signal is utilized to compute the diffusion coefficient and particle size. Usually, a gray filter is positioned between the laser and the cuvette to reduce the incident laser light. The filter parameters can either be modified automatically by the instrument or manually by the user. When measuring turbid samples, the detector would be unable of processing the number of photons. In order for the detector to obtain a sufficient but manageable signal, the laser light must be attenuated. [55]

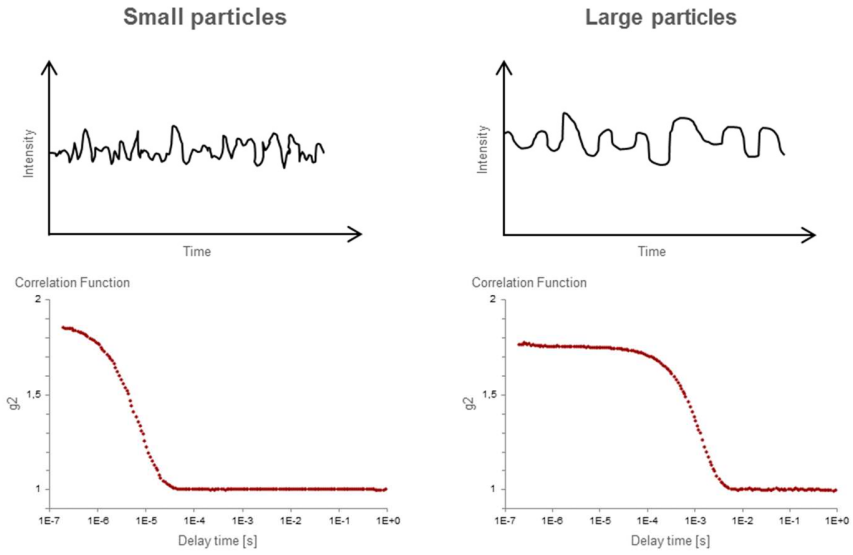


**Figure 25: Intensity and Correlation of large and small particles [55]**

Over a period of time, the dispersed light is measured in order to monitor the movement of the particles. The intensity of the scattered light fluctuates over time and is not constant. Smaller, faster-moving particles exhibit more rapid fluctuations than larger particles. On the other hand, the amplitudes between the highest and minimum scattering intensities are greater for larger particles. At general, the correlation function describes the length of time a particle remains in the same location inside the sample. Initially, the correlation function is linear and nearly constant, signifying that the particle is at the same place as before. Later, an exponential decline of the correlation function can be observed, indicating that the particle is in motion. If there is no resemblance to the initial location, the correlation function returns to its linear form. The baseline refers to this portion of the correlation function. The decay of the correlation function includes information regarding size-dependent mobility. The decay is an indirect estimate of the time required for the particles' relative locations to change. Small particles move rapidly, therefore decay is also rapid. Larger particles travel more slowly than smaller ones, delaying the depreciation of the correlation function. In reality, the correlation function is a mathematical representation of the dispersed light's variations. It is employed to calculate the translational diffusion coefficient. To accomplish this, the intensity of scattered light at time t is compared to the intensity of the identical intensity trace moved by the delay time ƈ (tau). It displays the same intensity trace as that which was captured during the measurement, shifted for various delay durations. Calculations are performed in real time and shown over a logarithmic time axis. Cumulant techniques are used to fit the correlation function, an ISO-standard procedure. The diffusion coefficient is derived from the cumulant algorithm, while the hydrodynamic diameter (particle size) is derived from the Stokes-Einstein equation, which has already been explained [55].

## 7.2 Pendant Drop Technique

The measurement of interfacial tension can be easily done by various measurement techniques such as shape measurements (rotating, rising or hanging or pendant drop method), mass measurements (weighed drop method) or force measurements (pull-off method). For this study, the pendant drop method was used for checking the purity of large microgels. The pendant drop is

a drop hanging from a needle within a liquid or gaseous bulk phase. The competition between surface tension or interfacial tension that maintains the drop and gravity that tend to make it falling determines the shape of a drop. In the pendant drop method, the surface tension or interfacial tension is computed from the shadow picture of a pendant drop by analyzing the drop's shape.

Due to the interfacial tension between the inner and outer phases, a rise in pressure is produced within the drop. The Young-Laplace equation describes the relationship between the pressure difference ΔP, the radii of curvature of the surface $r_1$ and $r_2$, and $\sigma$ the interfacial tension.

$$\Delta P = \sigma . \left[ \frac{1}{r_1} + \frac{1}{r_2} \right] \qquad (14)$$

The weight of the drop causes a hydrostatic pressure inside the drop, which changes the main radii of curvature ($r_1$ and $r_2$) and makes the drop look different. As the hydrostatic pressure changes with height, so does the shape of the drop interface.

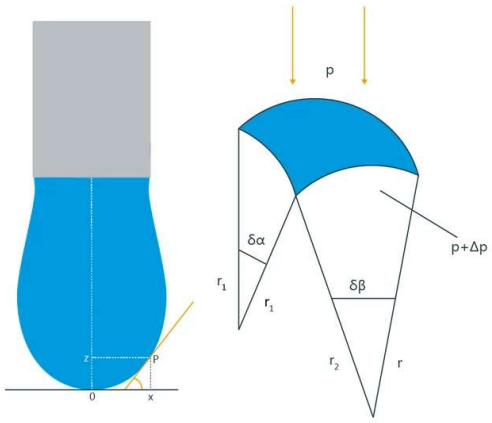


**Figure 26: Working Principle of Pendant Drop Method [56]**

This makes the "pear shape" that is typical of a pendant drop as seen in figure 26. The ratio between the weight of the drop and its surface tension shows how far away it is from a perfect sphere. If you know how much denser one phase is than the other, you can use the shape of the drop to figure out the surface tension.

Before measuring a drop, the size of the video image is taken into account. This lets you know how big the drop really is. The shape of the drop is then worked out by using greyscale analysis on a video of the dosed drop. Then, a numerical method is used to change a shape parameter called B until the shape of the calculated drop matches the shape of the real drop. The density difference and the changed B parameter are used to figure out the interfacial tension.[56]

## 7.3 Optical Microscope

Optical microscopes perform the following two primary functions:

- Creating a magnified image of a specimen
- An example of a specimen being illuminated

There are three essential tasks to creating a magnified image: "obtaining a clean, sharp image," "changing a magnification," and "putting it into focus.". The term "observation optical system" refers to an optical system used to carry out these duties. A specimen can be illuminated in three ways: by "supplying light," "gathering light," and "varying the intensity of that light," respectively. Illumination optical systems are designed to perform these functions. Another way to put it is that a specimen (specimen) is projected through an optical system and the projection picture is then shown to the observer's eyes (or a CCD). The figure 27 demonstrates about the optical microscope. [71]

**Figure 27: Optical Microscopes [71]**

While a light source emits light, the illumination optical system successfully collects and directs the light toward the specimen. An optical microscope's observation and illumination optical systems are arranged in the manner seen in the picture below. At contrast to an upright microscope, the arrangement relationship between the optical systems is reversed when using an inverted microscope in the specimen's center. [71]

# III Results

## 1. Study of Microgels

### 1.1 Study of Surface Tension

According to the protocol, large microgels are washed by centrifugation cycles following synthesis. At the end of the fifth cycle, the supernatant was recovered and its surface tension was measured using the pendant drop method for brief periods of time (about 100 s). When the surface tension of the supernatant is approximately equal to that of water, the microgels are considered washed with regard to the synthesis residues containing surfactant properties. In this instance, however, it was determined that five cycles of centrifugation-redispersion were insufficient to achieve the surface tension of pure water, and gave approximately value of 42 mN/m (Figure 28). Thus, two additional cycles of centrifugation were performed. After the seventh cycle, the same surface tension as pure water (approximately 72 mN/m) was observed in all the cases of large microgels, indicating that the microgels were completely purified. The graph represents about the behavior of surface tension with respect to cycles of centrifugation. After washing, there is no other species than microgels in the suspension able to adsorb at the interface.

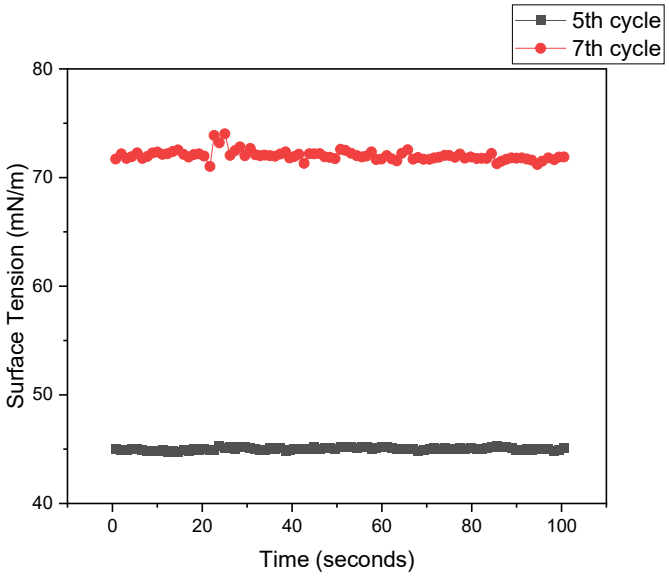


**Figure 28: Evolution of Surface Tension (after 5th and 7th cycle of centrifugation) as a function of time**

## 1.2 Study of Hydrodynamic Diameter

The purified microgels were then analyzed by Dynamic light scattering to determine the hydrodynamic diameter in a range of 15 to 55 °C. The study of the evolution of the diameter of the microgels as a function of temperature showed that whatever their size, their cross-linking rate, the microgels maintained their sensitivity to temperature with a VPTT of about 32°C. For a given type of microgels (in terms of size), the hydrodynamic diameters in the swollen (25°C) and contracted (50°C) states were noted in table 1. Microgels containing 1 % BIS had a polydispersity index below 0.1, which indicated good size homogeneity and the presence of only one component in solution. Two batches of microgels (large microgels) had almost the same hydrodynamic diameter in solution. Their behavior is shown in figure 29 below:

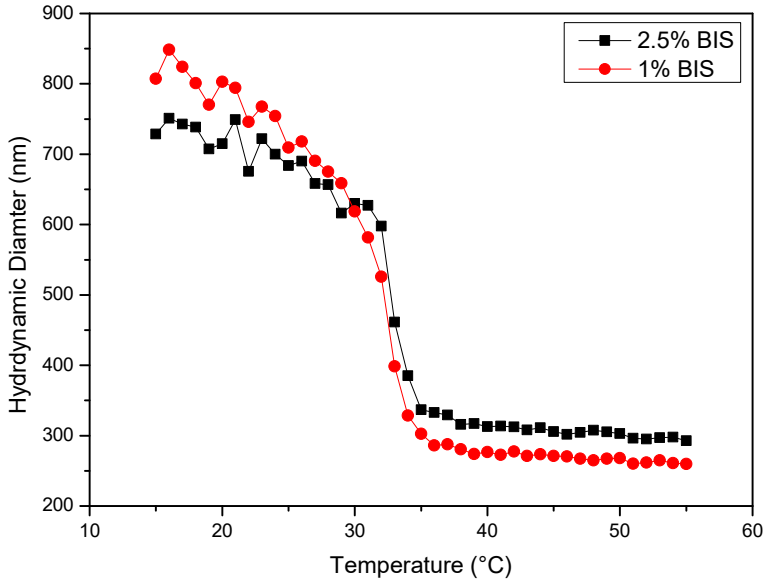


**Figure 29: Evolution of Hydrodynamic Diameter as a function of temperature in large microgels**

Two batches of small microgels were prepared, and their hydrodynamic diameters showed the same behavior but there is a slight increase in width of the phase transitions as compared to large microgels because of the size effect. Microgels had a polydispersity value of less than 0.1 in both cross-linking densities, indicated excellent size homogeneity and the existence of a single component in solution. The behavior is stated in figure 30.

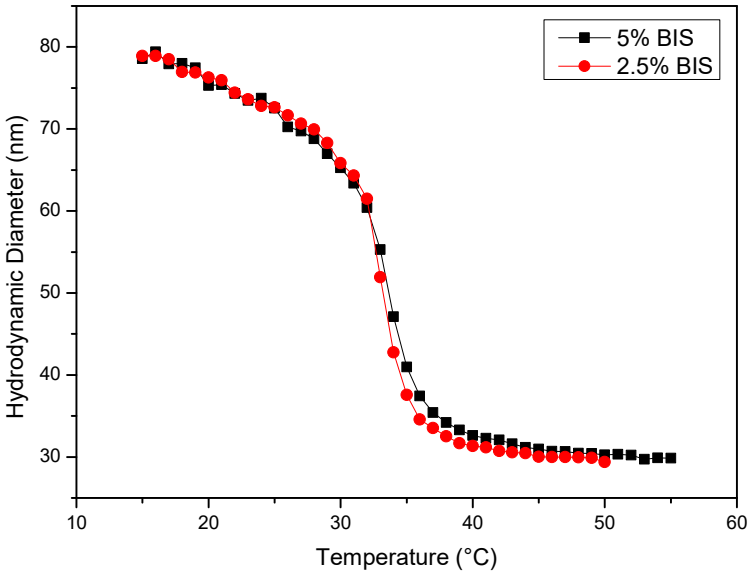


**Figure 30: Evolution of Hydrodynamic Diameter as a function of temperature in small microgels**

**Table 1: Hydrodynamic diameter at 25 and 50°C of the synthesized microgels with their respective PDI (Polydispersity Index) in brackets**

| Type of Microgels | BIS % Microgels | Hydrodynamic Diameter (25 °C) (nm) | Hydrodynamic Diameter (50°C) (nm) |
|---|---|---|---|
| Large | 1 | 709 (0.072) | 268 (0.053) |
| | 2.5 | 722 (0.195) | 292 (0.115) |
| Small | 2.5 | 72 (0.046) | 29 (0.042) |
| | 5 | 73 (0.064) | 30 (0.055) |

## 2. Study of Emulsions

### 2.1 Determination of Limited Coalescence Region

One of the main characteristics of Pickering emulsions is the high anchoring energy of the particles at the interfaces, which causes the phenomenon of limited coalescence. A low particle concentration, it is possible to directly relate the average drop size, D, to the quantity of particles (the number of particles), and their coverage rate at the interface. In order to get an idea of the microgel packing at the interface, a systematic study was carried out with the different synthesized microgels. The evolution of the inverse of the mean drop diameter (1/D) as a function of the concentration of particles. In case of both set of microgels (large and small), the inverse of the

droplet diameter was directly proportional to the amount of microgels initially introduced into the system. Linearity was only observed at low initial particle concentrations and beyond this domain, the emulsions become polydisperse and excess microgels were observed in the aqueous phase. It could be noticed that, for the same formulation route, the extent of the limited coalescence domain was very similar with the increase of the cross-linking rate as showed in figure 31 and 32 below. The macroscopic images of these emulsions are included in Annex-1.

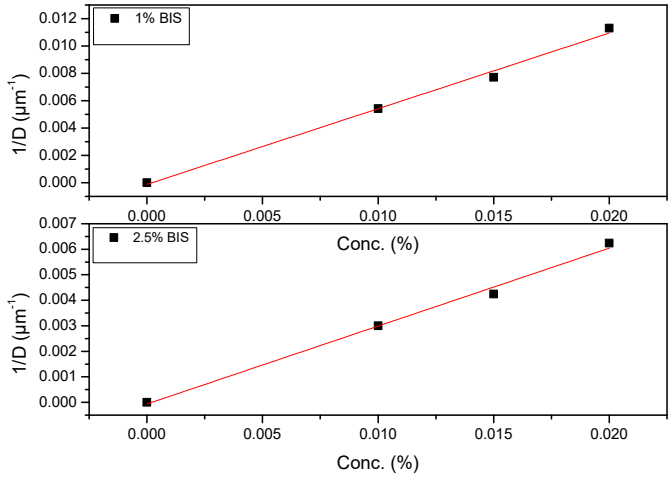


**Figure 31: Linear Domain of Limited Coalescence Curve for large microgels of emulsions prepared using PDMS and large axis**

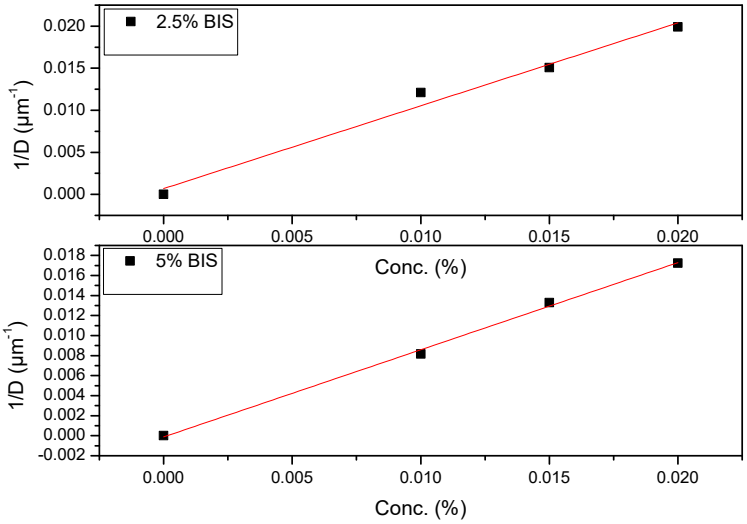


**Figure 32: Linear Domain of Limited Coalescence Curve for small microgels of emulsions prepared using PDMS and large axis**

As previously stated, the linear domain exhibited no excess of microgels in the continuous phase. In this range, all microgels are assumed to be adsorbed at the interfaces. The limited coalescence procedure can be used to determine the surface coverage C. This was be done by plotting the graph between 1/D where D is the average surface diameter (Sauter) of the drop's vs $Seq/6V_d$ where $V_d$ is the volume of the dispersed phase and the amount of interface covered is estimated by considering the microgels as spherical particles and taking into account their equatorial surface, $S_{eq} = n\pi\,(\frac{d_{25°C}}{2})^2$ where $d_{25°C}$ is the hydrodynamic diameter of the microgels in dispersion at 25°C and n is number of microgels in order to normalize the parameters governing the microgels which results in getting precise value of C. Then the slope is equal to 1/C presented in figures 33 and 34 and their values are mentioned in table 2.

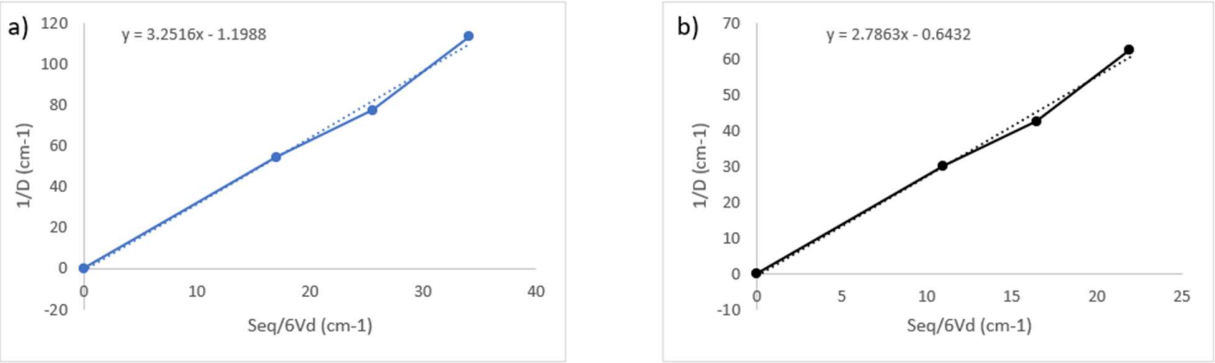


**Figure 33: Evolution of inverse of Diameter (1/D) as a function of Surface of equatorial region ($S_{eq}$) and $6V_d$ for large microgels of emulsions prepared using PDMS and large axis a) 1% BIS and b) 2.5% BIS**

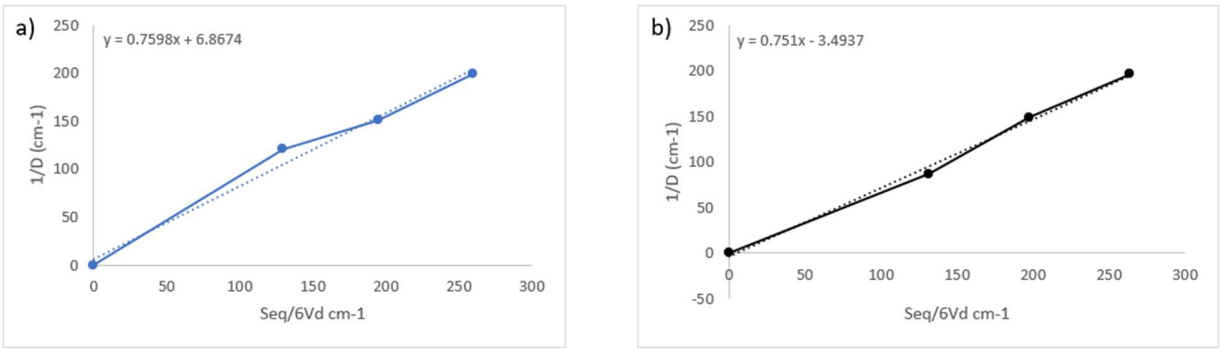


**Figure 34: Evolution of inverse of Diameter (1/D) as a function of Surface of equatorial region ($S_{eq}$) and $6V_d$ for small microgels of emulsions prepared using PDMS and large axis a) 2.5% BIS and b) 5% BIS**

The values of surface coverage of different systems of microgels are mentioned in the table 2 below:

**Table 2: Surface coverage values C deduced from the preceding graphs for PDMS-in-water emulsions prepared with the large axis**

| Type of Microgels | BIS % Microgels | Surface Coverage |
|---|---|---|
| Large | 1 | 0.31 |
| | 2.5 | 0.36 |
| Small | 2.5 | 1.31 |
| | 5 | 1.33 |

The preceding table demonstrated that surface coverage (C) is dependent of size of microgels. In the case of large microgels, surface coverages of 0.31 and 0.36 were observed for both densities of cross-linking. It indicated that the microgels were stretched (flatten) at the interface between oil and water. In fact, a number less than 0.9 indicates that the microgels occupy a larger surface at the interface than their equatorial plane, as calculated from the hydrodynamic diameter in the aqueous solution. Surprisingly, the surface coverage of the small microgels was 1.5 %, a figure far greater than the 0.9 indicated in the table 2. Due to the presence of a monolayer of particles, as in the case of small microgels, the microgels are compressed at the interface and occupy a lower surface than their initial equatorial plane. [43]

**Table 3: Surface coverage values C for PDMS-in-water emulsions prepared with the small axis and large axis**

| Type of Microgels | BIS % Microgels | Axis used for Emulsification | [Surface Coverage] C (%) |
|---|---|---|---|
| Large | 1 | Large (High Shear Rate) | 0.31 |
| | | Small (Low Shear Rate) | 0.45 |
| | 2.5 | Large (High Shear Rate) | 0.36 |
| | | Small (Low Shear Rate) | x |
| Small | 2.5 | Large (High Shear Rate) | 1.31 |
| | | Small (Low Shear Rate) | 1.66 |
| | 5 | Large (High Shear Rate) | 1.33 |

| | | | |
|---|---|---|---|
| | | Small (Low Shear Rate) | 1.99 |

Additionally, emulsification energy had an effect on surface coverage as described in table 3. In case of small microgels, for both cross-linking densities, the surface covered was less when the shear rate was high i.e., 0.31 in comparison to surface coverage got from emulsions prepared using less shear rate i.e., 0.45 due to the fact that less shear rate results in flattening of microgels at oil/water interface. It specified that the microgels were stretched at the interface between oil and water. Similarly, the surface coverage of microgels emulsified at the lowest shear rate was higher in case of small microgels as shown in the table 3 in both cross-link densities due to the compressibility at oil/water interface. Due to the small size microgels' capacity to induce high surface coverage and high interfacial connection, an interface was more elastic and better able to resist bridging and destabilization [47].

## 2.2 Study of Optical & Compression Behavior

The oil-in-water emulsions used in this study had a microgel concentration of 0.02 percent, which was chosen after analyzing the limited coalescence regions of the emulsions due to the irreversible microgel anchoring. The oil used in all cases was PDMS; however, Dodecane was also used to compare the nature of oil. Except for when comparing the effect of emulsification energy, emulsions were prepared using the large axis. The graphs explaining the compression behavior are in terms of the osmotic pressure ($\pi$) as a function of the droplet volume fraction, which was then normalized by the Laplace half-pressure $\gamma/R$, where $\gamma$ is the surface tension of the microgel suspension at the oil interface as given in figures 35 and 36 and R is the average radius of the droplets obtained from diameters mentioned in Table 4 for PDMS and Table 6 to Dodecane.

As it has been previously shown the surface tension in microgels do not depend on the microgels size, neither on their cross-linking density, neither on their concentration but it could be affected by the oil nature [82]. This is the reason why, adsorption kinetics of large microgels were measured at the oil/water interface at room temperature ($T \approx 22°C$), respectively (for both Dodecane and PDMS). These data are necessary for the normalization. For measurements at the oil/water

interface, a drop of microgel dispersion at a concentration of 0.5% is formed at the end of a needle dipped into a vessel containing purified dodecane/PDMS due to the fact that the adsorption kinetics are faster as the microgel concentration increases.

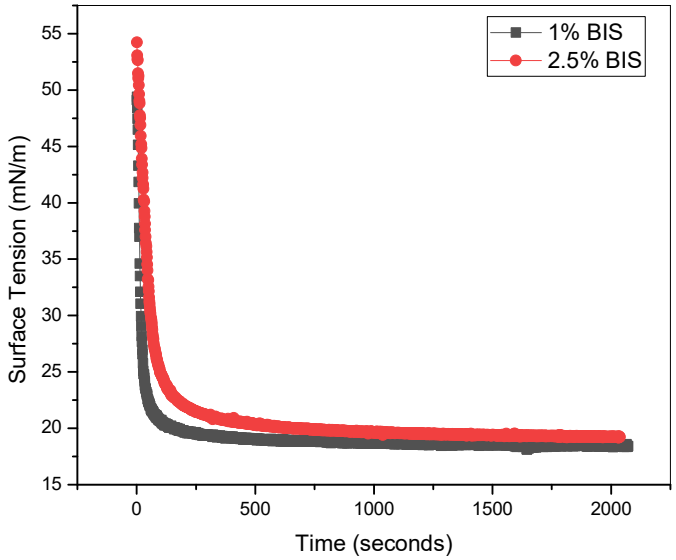


**Figure 35: Evolution of Surface Tension of Dodecane/Water interface v/s time**

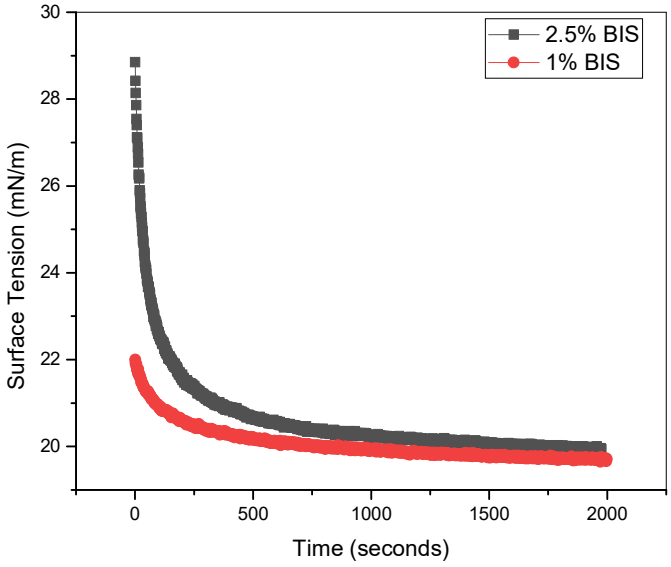


**Figure 36: Evolution of Surface Tension of PDMS/Water interface v/s time**

Figure 35 and 36 showed that the adsorption kinetics were similar, with the difference residing in the initial surface tension values due to the differences in theoretical interfacial tension values between the PDMS/water interface and the dodecane/water interface. Nevertheless, the

similarities observed between the two interfaces indicated that the adsorption phenomena at these two interfaces were comparable. The findings showed that after 2000 s, no matter what type of microgel and oil is utilized, the same tension plateau value of about 20 mN/m in case of PDMS and 19 mN/m in case of Dodecane.

### 2.2.1 Effect of Microgel's Cross-Linking Density

Optical microscope observations revealed those emulsions prepared with less crosslink microgels were less flocculated than those prepared with more crosslink microgels. A significant increase in emulsion's drop size and flocculation (in case of large microgels) was observed as the cross-link percentage increased as mentioned in figures 37 and 38 and table 4 below.

**Table 4: Drop Diameter for PDMS-in-water emulsions prepared with the large axis**

| Type of Microgels | BIS % Microgels | Axis Used for Emulsification | Drop Diameter measured (μm) | PDI (Polydispersity Index) |
|---|---|---|---|---|
| Large | 1 | Large | 88.34 | 0.09 |
| | 2.5 | | 160.16 | 0.17 |
| Small | 2.5 | | 50.25 | 0.04 |
| | 5 | | 58.35 | 0.06 |

In case of large microgels,

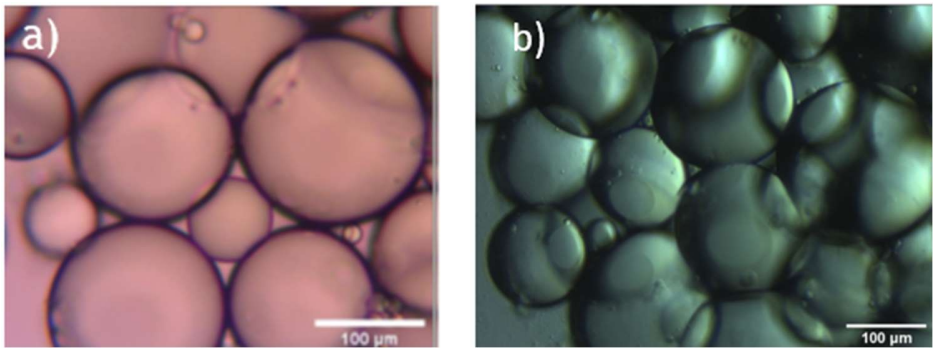


**Figure 37: Emulsions prepared by large microgels using large axis and PDMS a) 1% BIS and b) 2.5% BIS**

In case of small microgels,

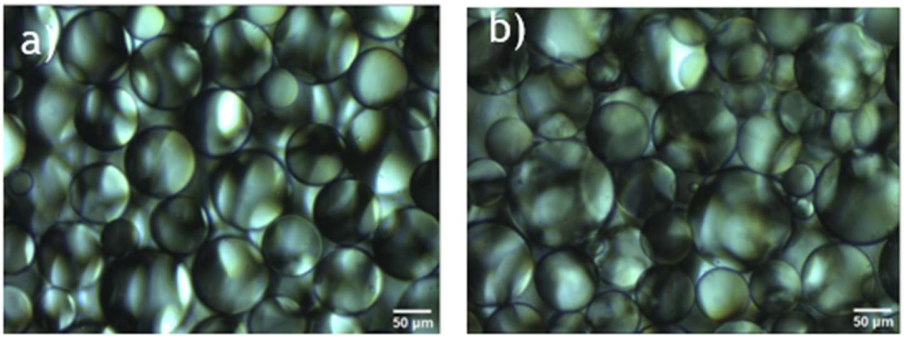


**Figure 38: Emulsions prepared by large microgels using large axis and PDMS a) 2.5% BIS and b) 5% BIS**

The information in the table below corresponds to the osmotic pressure of emulsions after compression (before breaking), in which it was observed that emulsions having less cross linking density had more limiting osmotic pressure as they can handle more compression without breaking due to their high stability in comparison with emulsions having high cross link density.

**Table 5: Osmotic pressure ($\pi^*$) before rupture of PDMS-in-water emulsions prepared with the large axis**

| Type of Microgels | BIS % Microgels | Osmotic Pressure ($\pi^*$) (Pa) before rupture |
|---|---|---|
| Large | 1 | 220 |
| | 2.5 | 77 |
| Small | 2.5 | 816 |
| | 5 | 405 |

Cross-linking density had a significant effect on the compression of the material, as shown in the graph cited below the osmotic pressure ($\pi$) normalized by the Laplace half-pressure $\frac{\gamma}{R}$ vs droplets volume fraction. In the case of large microgels, emulsions prepared with 1% BIS can be compressed up and get higher droplets volume fraction (0.71) than those prepared with 2.5% BIS (0.63) due to the presence of less flocculation, making them more resistant to breakage as mentioned in figure 39.

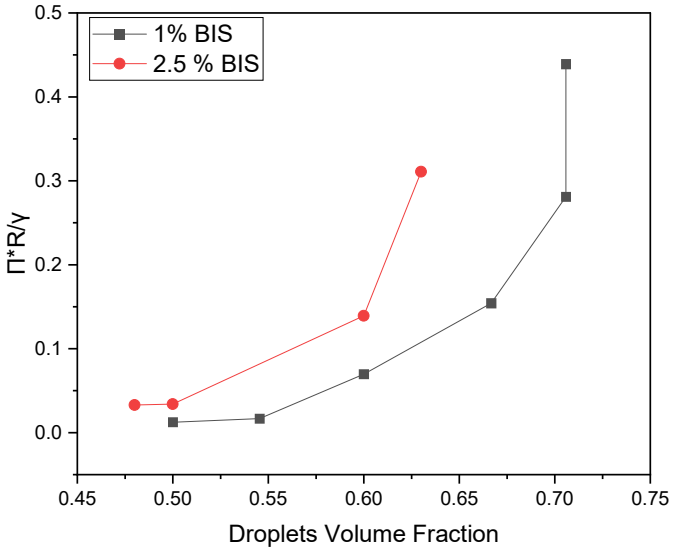


**Figure 39: Evolution of volume fraction in case of large microgels with respect to $\pi^*\frac{\gamma}{R}$ of emulsions prepared using large axis and PDMS**

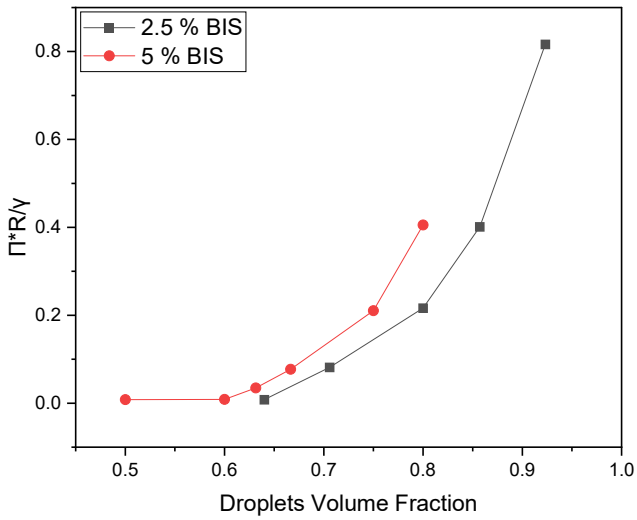


**Figure 40: Evolution of volume fraction in case of small microgels with respect to π*γ/R of emulsions prepared using large axis and PDMS**

Small microgels exhibited the same behavior as emulsions prepared with 5% BIS had a lower oil volume fraction (0.8) than emulsions prepared with 2.5% BIS (0.92), due to high interfacial packing that provides greater compressibility and rupture resistance as shown in figure 40.

### 2.2.2 Effect of Microgel size

The macroscopic view of emulsions revealed that, for the same particle concentration and dispersed phase fraction, the emulsions become more flocculated as the size of the microgels increases. In particular, the emulsion obtained with small size microgels containing 2.5% BIS is not at all flocculated and flows very easily, in contrast to emulsions formulated with large size microgels containing 2.5% BIS, which form a rigid block conforming to the shape of the vessel, as depicted in the figure 41 below.

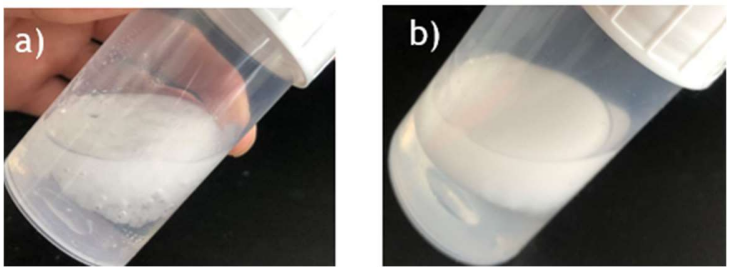


**Figure 41: Macroscopic images of emulsions prepared using large axis and PDMS a) 2.5% BIS large microgels b) 2.5 % BIS small microgels**

Optical Microscopy revealed that emulsions made with small microgels have smaller drop diameters and are more stable than emulsions made with large microgels as revealed in figure 42 below. This is because the cross-linker distribution in small microgels is more homogeneous, and the core-shell morphology is less prominent. Microgels with a smaller diameter cover more of the oil-water interface with greater density and uniformity as a result of the decreased deformation gradient of adsorbed microgels. Another advantage of small size microgels is their increased mobility and ability to rearrange themselves, making it possible for the interfaces to better withstand mechanical stresses. Due to all of these features, emulsions become easier to handle and have less flocculation.

In case of large microgels, their internal structure grows more complex and so does the polymeric layer they form. The absence of a uniformly dense layer promotes the formation of bridges between adjacent drops, resulting in flocculated and thus less manageable emulsions. In conclusion, the emulsion characteristics largely depend on the particle size of the stabilizer: as the

particle size increases, dispersed droplets and fluid emulsions evolve into extremely adherent drops and flocculated emulsions.

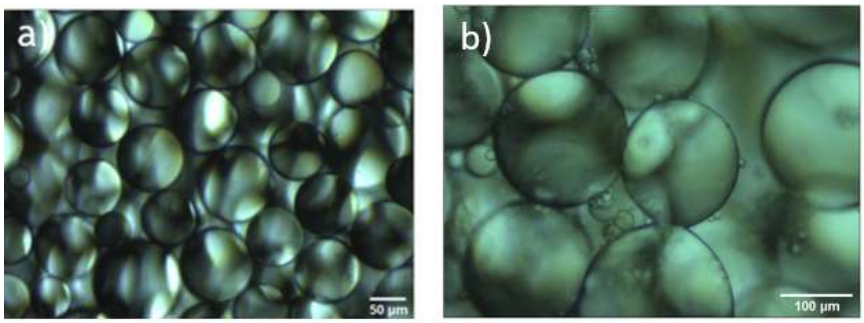


**Figure 42: Emulsion prepared by large axis and PDMS a) 2.5% BIS small microgels b) 2.5% BIS large microgels**

A compression study with the help of centrifugation was conducted to determine the effect of microgel's size by plotting graph between the limiting osmotic pressure normalized by the Laplace half-pressure $\frac{\gamma}{R}$ and droplets volume fraction. Comparing the compression behavior revealed that emulsions prepared with large microgels had a lower volume fraction and osmotic pressure than emulsions prepared with small microgels. This is due to the high adhesion between drops, which resulted in fragile emulsions that are easily ruptured by mechanical means. In the case of large microgels, the emulsions reached a maximum oil volume fraction of 0.70 and a limited osmotic pressure of 220 Pa (given in table 5), whereas in the case of small microgels, the maximum volume fraction was 0.92 and the osmotic pressure was 816 Pa (given in table 5) as a result of the homogenous packing of microgels at the interface, which provides a high resistance to breakage as shown in figure 43.

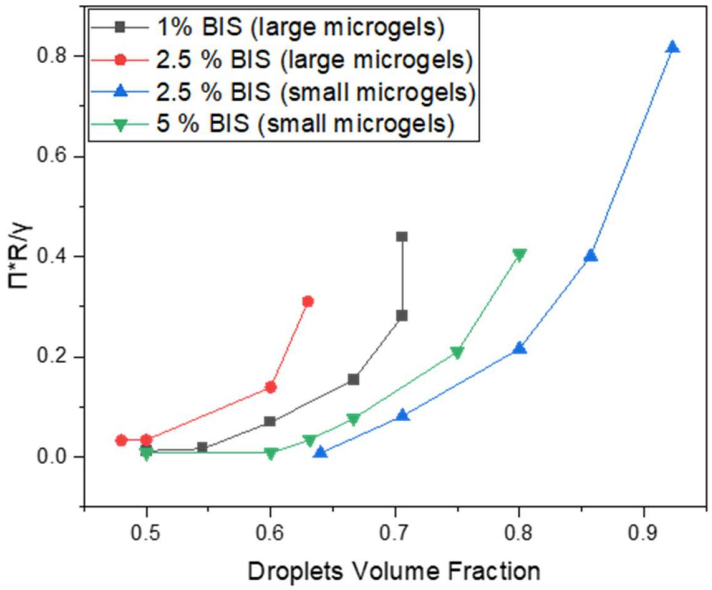


**Figure 43: Evolution of volume fraction of different set of microgels with respect to $\pi^*\frac{\gamma}{R}$ of emulsions prepared using large axis and PDMS**

### 2.2.3 Effect of Emulsification Energy

It was necessary to use two different-sized axes on the rotor stator in order to alter the emulsion's energy distribution. Large rotor head was utilized for strong shear rate, whereas smaller rotor head was employed for reduced shear rate. The microscopic characteristics of the emulsions were affected by the emulsification energy utilized. High-energy emulsions were stabilized by microgels that have been flattened, and their drops were flocculated by bridging. Low-energy emulsions were stabilized by compressed microgels, and there was no bridging. A high shear emulsification process promotes the spreading of microgels at the interface. As a result, the process of drop coalescence was restricted at an early stage, resulting in a lower interfacial microgel density. The microgels' lateral deformation results in a poor overlap of their side dandling chains. This resulted in approaching drops favors bridging events and caused emulsion flocculation. Using a low shear emulsification process, on the other hand, did not promote microgel spreading at the interface. Due to drop coalescence following the termination of emulsification, the reduction in interfacial surface area concentrates the microgels, which were ultimately constrained by their resistance to compression. This process produced a high density of compressed microgels at the interface, which promotes a significant overlap of their lateral chains. As a result, the resistance is

sufficient to prevent the formation of bridges: drops remain distinct and flow freely. Moreover, it demonstrated a substantial difference in the average drop diameter between the emulsions formed with high and low shear, confirming the differences in dispersion state as mentioned in figure 44 below.

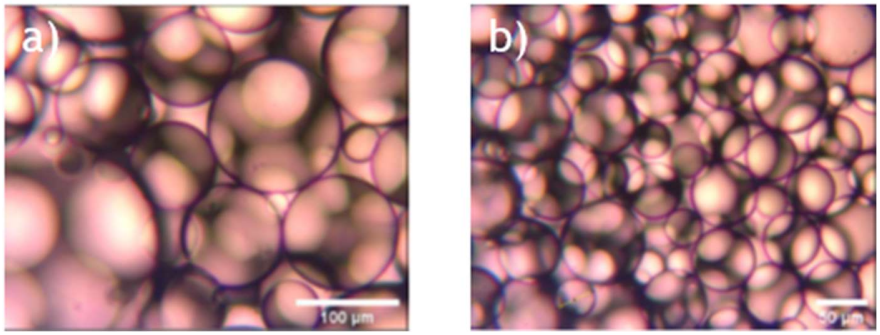


**Figure 44: Emulsions prepared using PDMS with 2.5% BIS small microgels a) Small axis b) Large axis**

To comprehend the influence of the emulsification process, a study of compression behavior was conducted. Due to the presence of more bridged drops, which resulted in fragile emulsions, the droplets volume fraction and osmotic pressure of emulsions prepared with a large axis were lower than those prepared with a small axis. Each of the graphs below (figure 45 and 46) provided an illustration of the size of microgels. In the case of large microgels (1% BIS), the maximum volume fraction attained by emulsions prepared with low energy was 0.85 and high osmotic pressure due to greater mechanical stability as a result of good interfacial packing of microgels at the oil interface, whereas emulsions prepared with high energy yielded low osmotic pressure as well as volume fraction of 0.70 because in this case the starting volume fractions below 0.635 which means that they were more flocculated due to which they were more susceptible to destabilization under compression. This behavior is shown in graph (figure 45 and 46) between the limiting osmotic pressure normalized by the Laplace half-pressure $\frac{\gamma}{R}$ v/s droplets volume fraction.

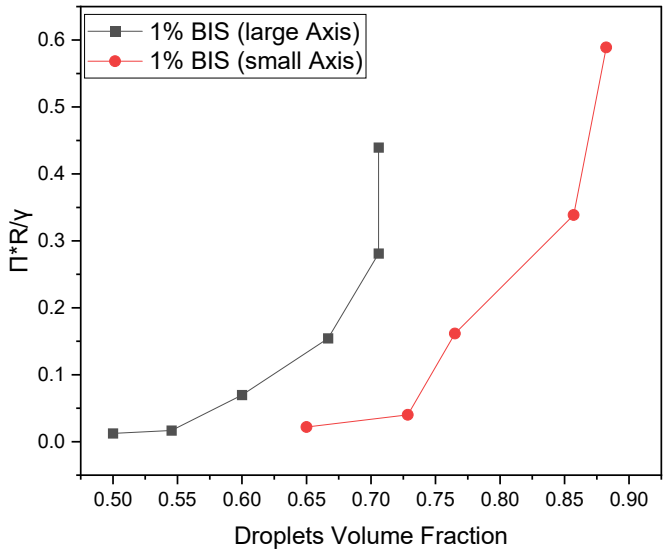


**Figure 45: Evolution of volume fraction in case of large microgels (1% BIS) with respect to π*γ/R of emulsions prepared using PDMS with large axis (black) and small axis (red)**

Small microgels (2.5 percent BIS) exhibited a similar behavior, with a volume fraction of 0.92 for emulsions prepared with a large axis (high energy), compared to 0.97 for emulsions prepared with a small axis, which are more stable and dispersed. The results are depicted in the figure 46 below.

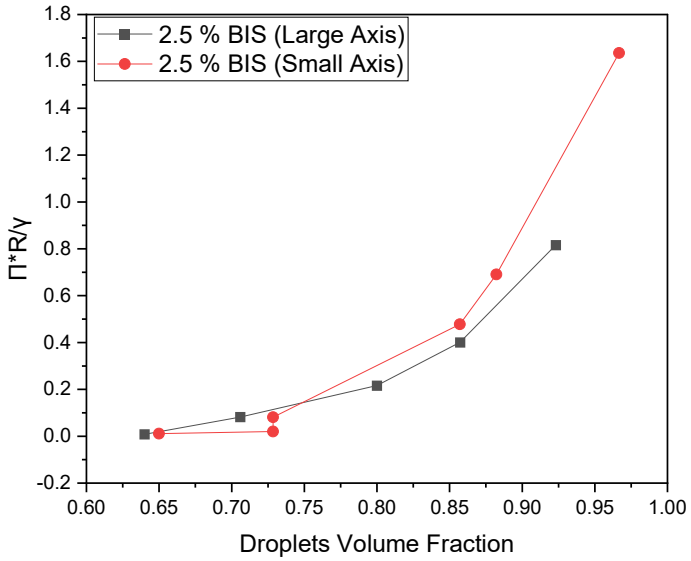


**Figure 46: Evolution of volume fraction in case of small microgels (2.5% BIS) with respect to π*γ/R of emulsions prepared using PDMS with large axis (black) and small axis (red)**

### 2.2.4 Nature of Oil

Before, the oil was PDMS. Experiments were also conducted with Dodecane as the oil phase to evaluate its effect. Through the use of an optical microscope, it was discovered that there was a correlation between the change in cross-linking density and the size of the microgels, i.e., with an increase in cross-linking density and microgel size, there was an increase in drop diameter and adhesion between drops, which led to a decrease in the instability of the emulsions, as shown in the images (figure 47 and figure 48) and table 6 below. Due to the small difference in viscosity between the used oil phases, the droplet diameters of these emulsions and the PDMS-prepared emulsion are very similar.

**Table 6: Drop Diameter for Dodecane-in-water emulsions prepared with the large axis**

| Type of Microgels | BIS % Microgels | Axis Used for Emulsification | Drop Diameter (μm) | PDI (Polydispersity Index) |
|---|---|---|---|---|
| Large | 1 | Large | 95.07 | 0.07 |
| | 2.5 | | 180.37 | 0.19 |
| Small | 2.5 | | 60.23 | 0.03 |
| | 5 | | 65.27 | 0.05 |

In case of small microgels,

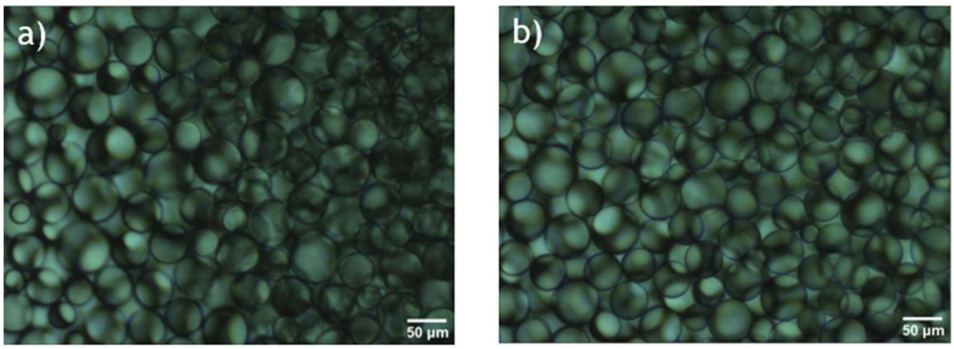


**Figure 47: Emulsions prepared using Dodecane with large axis in case of small microgels a) 2.5% BIS and b) 5% BIS**

In case of large microgels,

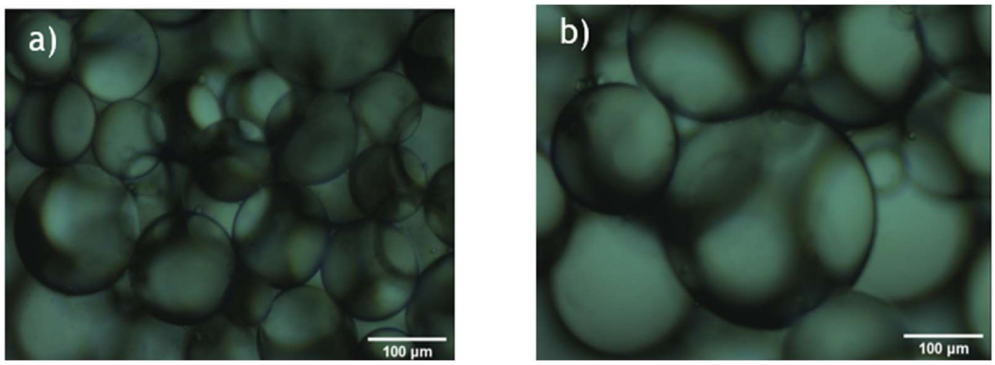


**Figure 48: Emulsions prepared using Dodecane with large axis by large microgels a) 1% BIS and b) 2.5% BIS**

A study was conducted to understand the effect of the oil phase on compression behavior. Due to the high-density difference and less polarity of dodecane compared to PDMS, the emulsion's droplets volume fraction and osmotic pressure were high (as osmotic pressure is directly dependent of density difference that is described in method part of compression) because of which these emulsions were more stable and more resistant to rupture under compression. In the case of large microgels (1% BIS), the maximum volume fraction attained by emulsions prepared was 0.75 and osmotic pressure was highest due to good interfacial packing of microgels at the oil interface, whereas emulsions prepared with (2.5% BIS) yielded low osmotic pressure as well as volume fraction because they were more delicate and prone to rupture under compression.

In the case of small microgels, the volume fraction was 0.88 for emulsions prepared with microgels containing 5% BIS, compared to 0.99 for emulsions prepared with microgels containing 2.5% BIS, which are well-dispersed and harder to break under compression. The results are depicted in graph between the limiting osmotic pressure normalized by the Laplace half-pressure $\frac{\gamma}{R}$ v/s droplets volume fraction in figure 49 below and the values of osmotic pressures are given in table 7.

**Table 7: Osmotic pressure ($\pi^*$) before rupture of Dodecane-in-water emulsions prepared with the large axis**

| Type of Microgels | BIS % Microgels | Osmotic Pressure ($\pi^*$) (Pa) before rupture |
|---|---|---|

| | | |
|---|---|---|
| Large | 1 | 893 |
| | 2.5 | 326 |
| Small | 2.5 | 3686 |
| | 5 | 1838 |

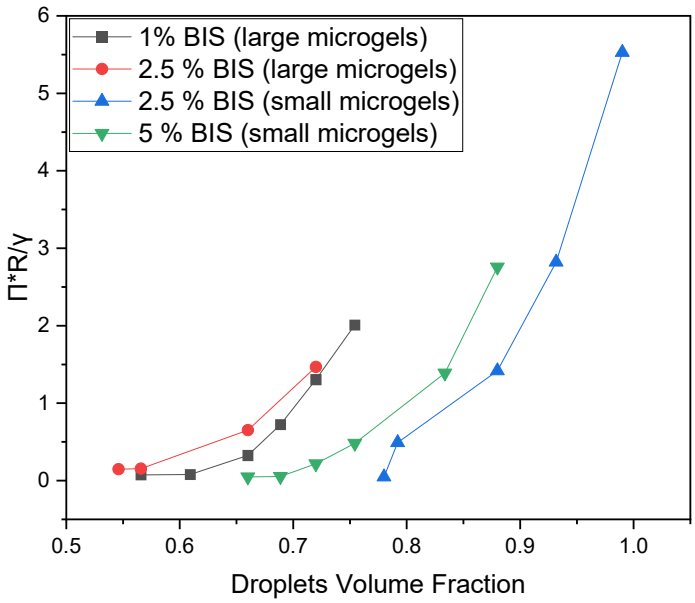


**Figure 49: Evolution of volume fraction of different set of microgels with respect to π*γ/R (in case of Dodecane) of emulsions prepared with large axis**

# IV Discussion of Results

The interfacial energy of emulsions determines their mechanical properties. Let's start with interfaces in equilibrium. A change in free energy occurs when an emulsion is subjected to a stress (such as osmotic or shear stress). For a monodisperse group of N droplets of radius R, the total interfacial area of the undeformed droplets is $S_0 = 4\pi NR^2$. If the emulsion is compressed up to $\varphi > \varphi_{rcp}$ $(\varphi_{rcp} = 0.635)$, each droplet is persistent against its neighboring droplets with flat facets. Therefore, the total surface area, S, becomes greater than $S_0$. The osmotic resistance is thus the derivative of the free energy F with respect to the total volume V at constant number of droplets:

$$\Pi = -\left(\frac{\partial F}{\partial V}\right)_N = -\left(\frac{\partial F}{\partial S}\right)_N * \left(-\left(\frac{\partial S}{\partial V}\right)_N\right) \quad (15)$$

The derivative of F with respect to S, $\sigma = \left(\frac{\partial F}{\partial S}\right)_N$,symbolizes the mechanical behavior of the surface and is equivalent to the interfacial tension, in the case of a surfactant covered interface. A similar method can be accepted for the bulk shear modulus. If the emulsion – already compressed to a surface S involves a small shear strain, Γ, the total interface rises quadratically with the strain – as shown by Princen [83]. The entire droplet surfaces $S+\frac{1}{2}\Gamma^2 = \frac{\partial^2 S}{\partial \Gamma^2}$. The bulk stress can be written as $\tau = \frac{1}{V} = \left(\frac{\partial F}{\partial \Gamma}\right)_N = \frac{\Gamma}{V}\left(\frac{\partial F}{\partial S}\right)_N = \frac{\partial^2 S}{\partial \Gamma^2}$. The shear modulus is specified by:

$$G = \frac{1}{V} = \left(\frac{\partial F}{\partial S}\right)_N = \frac{\partial^2 S}{\partial \Gamma^2} \quad (16)$$

Hence, both the osmotic resistance and the bulk shear modulus can be stated as products of two independent parameters, the derivative of the free energy with respect to the quantity of interface and a geometrical factor $\left(\frac{\partial S}{\partial V}\right)_N$ and $\frac{\partial^2 S}{\partial \Gamma^2}$ representing the outcome of a compression and of a strain correspondingly. From the results of Mason et al. [83] it is easy to conclude the φ dependence of these two functions:

$$\left(\frac{\partial S}{\partial V}\right)_N = \frac{1.7\varphi^2(\varphi_{rcp} - \varphi_c)}{R} \quad (17)$$

$$\frac{\partial^2 S}{\partial \Gamma^2} = 0.57 S_0 \varphi(\varphi - \varphi_{rcp}) \quad (18)$$

It is interesting to note that $\left(\frac{\partial S}{\partial V}\right)_N \approx -\frac{1}{V}\frac{\partial^2 S}{\partial \Gamma^2}$. This is a significance of the fact that G and Π were found nearly equal for φ < 95% in surfactant-stabilized emulsions [84]. Assuming that the factors $\left(\frac{\partial S}{\partial V}\right)_N$ and $\frac{1}{V}\frac{\partial^2 S}{\partial \Gamma^2}$ are only geometrical and independent of the interface nature, following equations (15) and (16), this should be identically obtained G ≈ Π, in solid-stabilized emulsions. Since in solid-stabilized emulsions, the interfaces cover particles with attractive interactions, they are probable to behave like 2D solids. Recall that the bulk elasticity derives mostly from the extension and shear of the interfaces and not from their bending, as the thickness of the interfaces

is relatively small relative to the radius of the droplets. Specifically, the ratio of the extensional energy to the buckling energy – for instance swelling a shell from R to R + δR is about $R^2/e^2$ where e is the thickness of the interface (of the order of the particle diameter) which is negligible compared to R. Following equations (15) and (18), the assumption of derivative of the free energy is done with the help of general relation:

$$\sigma = \left(\frac{\partial F}{\partial S}\right)_N = \frac{\Pi R}{1.7\varphi^2(\varphi - \varphi_{rcp})} \quad (19)$$

Actually, σ measures the bi-dimensional (2D) stress of the interface.

By integrating equation (17), the calculation of the relative strain $\varepsilon$ is:

$$\frac{S - S_0}{S_0} = \int_{S_0}^{S} \frac{dS}{S_0} = 0.3\,(\varphi - \varphi_{rcp})^2 = \varepsilon \quad (20)$$

For all the data with a volume fraction (φ) of emulsions greater than 0.635, the stress vs. strain curve is drawn because the drops of these emulsions have attained random close packing and can be compressed, demonstrating the elastic behavior of emulsions.

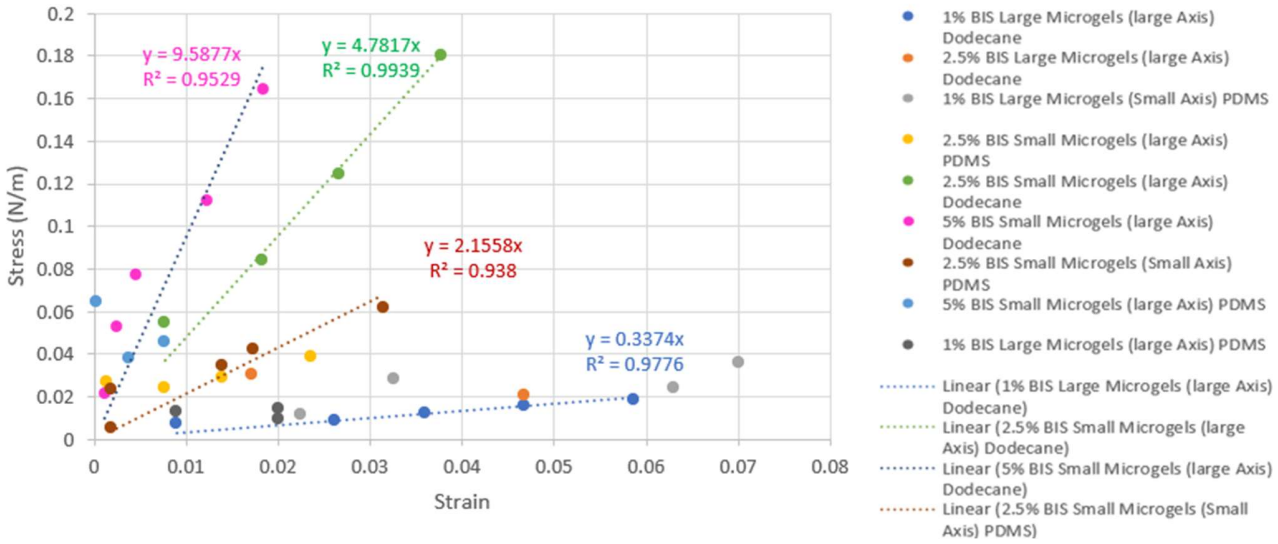


**Figure 50: 2D Stress vs Strain curves for all set of emulsions**

It was often believed that the mechanical behavior of the interface could be considered a constant at any given time (as we did ourselves when normalizing the pressure). This is true for surfactant stabilized interfaces, in which the interfacial tension accurately depicts the interface. This has also been proven for emulsion stabilized by non-deformable hard particles [20]. In the latter scenario, the constant stress that needs to be overcome in order to deform the drops corresponded to a plastic yield stress that originated from strong attraction between the adsorbed hydrophobically modified silica particles. This stress needed to be overcome in order to deform the drops [20]. The graph (Figure 50) exhibits a linear connection between stress and strain that is characteristic of elastic behavior. This demonstrates that microgels-stabilized interface behaves elastically. It appears that the cross-linking density is the most deciding parameter, and in the case of 2.5 percent, the nature of the oil also seems to affect the compression elastic moduli of the interface that can be extracted. Both of these factors may have an effect on the behavior.

**Table 8: 2D Stress and Strain values of emulsions showing linear behavior**

| Emulsions | 2D Stress modulus (N/m) | Strain before rupture |
|---|---|---|
| 5% BIS Small Microgels Dodecane (Large Axis) | ~ 10 | 0.02 |
| 2.5% BIS Small Microgels Dodecane (Large Axis) | ~ 5 | 0.04 |
| 2.5% BIS Small Microgels PDMS (Small Axis) | ~ 2 | 0.03 |
| 1% BIS Large Microgels Dodecane (Large Axis) | ~ 0.3 | 0.06 |

The more cross-linked microgels lead to stiffer and less deformable interfaces while the less cross-linked microgels covered interfaces are less elastic but more much more deformable. This is likely the reason of emulsions that better withstand mechanical disturbances.

# V Conclusions

In this study, Pickering emulsions were successfully prepared by stabilizing oil-in-water emulsions with pNIPAM microgels. Controlling various parameters, such as size and cross-linking density, had led to the synthesis of microgels and the preparation of controlled emulsions with a narrow size distribution. The range of limited coalescence was then determined for microgels of various sizes and cross-linking rates, allowing the study of emulsions with low polydispersity and the indirect study of packing of microgels at interface was effectively done by using optical microscopy. The compression behavior of the emulsions was then determined by measuring the relationship between osmotic pressure and droplet volume fraction after centrifugation. This was accomplished by examining the effect of microgel cross-linking density and size, the nature of the oil phase, and formulation process (emulsification procedure) on the emulsion's flocculation state and compression behavior which are described as follows:

- Influence of cross-linking density: It was found that emulsions with a lower cross-linking density had a greater limiting osmotic pressure and droplets volume fraction than emulsions with a higher cross-linking density. This shows that emulsions with a lower cross-linking density are more stable and are able to withstand a greater amount of compression without breaking.

- Influence of microgel's size: It was revealed that emulsions made with large microgels had droplet volume fraction and osmotic pressure that are lower than those made with small microgels. This is likely because of the strong adhesion that exists between the drops, which leads to emulsions that are extremely fragile and can be easily broken by mechanical methods.

- Influence of emulsification process: It was discovered that emulsions prepared with a low shear rate are less susceptible to destabilization under compression than emulsions prepared with a high shear rate. This is because the low shear emulsification process capacity to induce high surface coverage and high interfacial connection, an interface was more elastic and better able to resist bridging and destabilization. Also, this method

generated a high density of compressed microgels near the interface, which facilitates a substantial overlap of their lateral chains. Therefore, the resistance is adequate to prevent the creation of bridges and mechanical failure.

- Influence of nature of oil: Emulsions produced with Dodecane are more stable and harder to break under compression because of the high density difference and less polarity of dodecane compared to PDMS. The droplets volume fraction and osmotic pressure are high (as osmotic pressure is directly dependent on density difference that is stated in the procedure section of compression) because these emulsions are more resistant to rupture under compression.

The results were interpreted in terms of the elasticity of the adsorbed particles interfaces because of the existence of interpenetrated particles leading to a linear connection between stress and strain that is characteristic of elastic behavior. As a result, small size microgels of the 2.5% BIS type appear to be the most suitable for obtaining non-flocculated and kinetically stable emulsions with the highest osmotic pressure and droplets volume fraction as well as linear behavior in interpretation which confirms the elastic behavior of the emulsion.

# VI EIT Chapter

Items such as chocolate mousse, milk, beer, mayonnaise, salad dressing, shaving foam, bubble bath, ointment, active ingredient cream, bitumen emulsions, road coating, and building sealants are all examples of products that include emulsified bitumen (mastic) and every single day, members of the general public put these foams and emulsions to use. The use of these systems is common in a variety of industrial applications. In the chemical, petrochemical, petroleum, food, agricultural, cosmetic, pharmaceutical, and veterinary industries, foams and emulsions are put to productive use. These metastable dispersed systems, which are used in the production of a wide variety of products, are characterized by the presence of two phases that cannot mix with one another. In the case of foams, these phases are liquid and liquid. Both liquid-on-liquid phases (as in the case of an emulsion) and liquid-on-gas phases are made more stable by the presence of surfactant molecules (in the case of a foam). On the market, there is an ever-growing demand for surfactants. According to the forecast, the global surfactants market is expected to grow from $41.22 billion in 2021 to 57.81 billion by 2028 at a CAGR of 4.9% between 2021 and 2028 [74]. On the other hand, it is essential to lessen the quantity of surfactant that is utilized in each of these applications. On the one hand, there are concerns over the environment and the safety of the customer. It is true that surfactants can be toxic and hazardous, not only to consumers but also to the environment. An alternative would be to produce foams and emulsions without using surfactants in the process. Over the course of the last few decades, there has been a revival in the research and development of particle-stabilized emulsions and foams. These systems, which also go by the name of the Pickering effect, are both interesting from an economic and environmental standpoint. On the other hand, in contrast to surfactants, which are in thermodynamic equilibrium at the interface, the produced systems are unusually stable over the course of time. This is due to the fact that the adsorption of particles at surfaces is irreversible. In contrast, given the current state of the economy and the environment, it would be desirable if there were solutions that were both less expensive and friendlier to the planet. In addition, a Pickering emulsion does not require the use of emulsifiers to be generated. In addition to this, the particles have a firm hold on the oil-water interfaces in a permanent manner. The development of a stiff barrier that prevents coalescence leads to the creation of emulsions that are exceptionally stable. If these concepts of thought were to be combined, it would be possible to make emulsions that are exceptionally stable

over the long term as a result of the Pickering effect without having to resort to the application of surfactants.

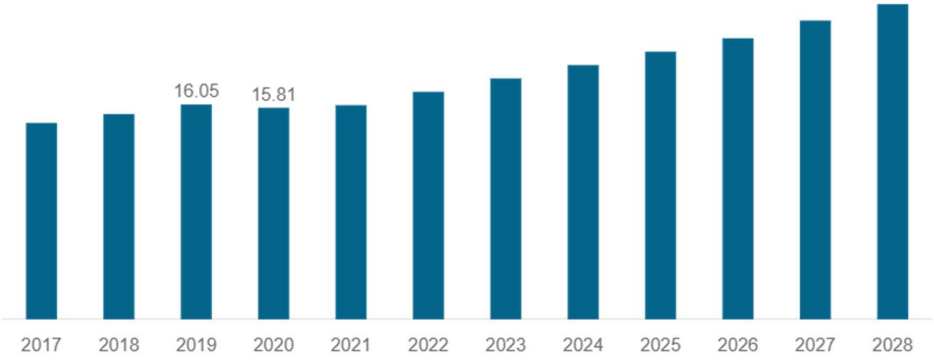


**Figure 51: Global Production of Surfactants (2017-2028) [74]**

# VII References


[1] https://goldbook.iupac.org/terms/view/E02065

[2] V. Schmitt, V. Ravaine, Surface compaction versus stretching in Pickering emulsions stabilised by microgels. Current opinion in Colloid & Interface Science, 532-541. 2013

[3] Yang, Yunqi & Fang, Zhiwei & Chen, Xuan & Zhang, Weiwang & Xie, Yangmei & Chen, Yinghui & Liu, Zhenguo & Yuan, Weien, An Overview of Pickering Emulsions: Solid-Particle Materials, Classification, Morphology, and Applications. Frontiers in Pharmacology, 2017

[4] W. Ramsden, Separation of solids in the surface-layers of solutions and 'suspensions'. Preliminary account. Proceedings of the Royal Society, vol. 72, n° 479, pp. 156-164, 1903.

[5] S. U. Pickering, Emulsions Journal of the Chemical Society, pp. 2001-2021, 1907.

[6] Y. Chevalier and M. Bolzinger, Emulsions stabilized with solid nanoparticles: Pickering emulsions» Colloids and Surfaces A: Physicochemical and Engineering Aspects, n° 439, pp. 23-34, 2013.

[7] D. Gonzalez Ortiz, C. Pochat-Bohatier, J. Cambedouzou, M. Bechelany, P. Miele, Current trends in pickering emulsions: Particle morphology and applications, Engineering (2020),

[8] Gibbs, J.W. The collected works of J.W. Gibbs. Longsmann, Green and Co., 1931.

[9] B. Le Neindre, “Surface and interfacial tensions” Engineering Techniques, 1993.

[10] B. Binks and J. Clint, “Solid wettability from surface energy components: Relevance to Pickering emulsions' Langmuir, vol. 18, p. 1270-1273, 2002.

[11] M. Destribats, S. Gineste, E. Laurichesse, H. Tanner, F. Leal-Calderon, V. Héroguez and V. Schmitt, “Pickering emulsions: What are the main parameters determining the emulsion type and interface properties?” Langmuir, vol. 30, p. 9313-9326, 2014.

[12] P. Finkle, H. Draper, and J. Hildebrand, "The theory of emulsification," Journal of American Chemical Society., vol. 45, p. 2780-8, 1923.

[13] M. Krapper, S. Nenov, R. Hachick, K. Müller and K. Müllen, “Oil-in-oil emulsions: a unique tool for the formation of polymer nanoparticles” Accounts of chemical research, vol. 41, no. 9, p. 1190-1201, 2008.

[14] B. Binks and T. Horozov, Colloidal particles at liquid interfaces, Cambridge University Press, 2006.

[15] P. Binks, “Multiple emulsions stabilized solely by nanoparticles.” At Proceedings of 3rd world congress on emulsions, Lyon, France, 2002.
[16] B. Binks and S. Lumsdon, “Effects of Oil type and aqueous phase composition on oil-water mixtures containing particles of intermediate hydrophobicity» Physical Chemistry Chemical Physics., vol. 2, p. 2959-2967, 2000.
[17] M. Destribats, “Emulsions stabilized by stimulable colloidal particles: Properties fundamentals and materials” PhD thesis at University of Bordeaux 1, Bordeaux, 2010.
[18] S. Levine, BD Bowen and SJ Partridge, “Stabilization of emulsions by fine particles I. Partitioning of particles between continuous phase and oil/water interface» Colloids and Surfaces, vol. 38, p. 325-343, 1989.
[19] R. Aveyard, B. Binks and J. Clint, “Emulsions stabilized solely by colloidal particles” Advances in Colloid and Interface Science, Vols. 100-102, p. 503-546, 2003.
[20] S. Arditty. Fabrication, stability and rheological properties of emulsions stabilized by colloidal particles. PhD thesis at the University of Bordeaux. 2004
[21] P. Pieranski, "Two-dimensional interfacial colloidal crystals" Physical Review Letters, vol. 45, pp. 569-572, 1980.
[22] R. J. Hunter, Foundations of colloid science, vol 1, Oxford, UK: Oxford University Press, 1986.
[23] T. N. Hunter, R. J. Pugh, G. Franks and G. J. Jameson, "The role of particle in stabilizing foams and emulsions" Advances in colloid and interface science, vol. 137, pp. 57-81, 2008.
[24] P.A. Kralchevsky, N. Denkov, Capillary Forces and Structuring in Layers of Colloid Particles. Current Opinion in Colloid & Interface Science. 6. 383-401. 2001
[25] Ostwald, W., Blocking of Ostwald ripening allowing long-term stabilization. Phys. Chem, .37: p. 385., 1901
[26] Leal-Calderon, F., V. Schmitt, and J. Bibette, Emulsion Science. Basic Principles. 2007: Springer. 227.
[27] M. Destribats, V. Schmitt. Soft microgels as Pickering emulsion stabilizers: role of particle deformability. Soft Matter, 7689-7698. 2011
[28] Wiley, R.M., Limited coalescence of oil droplets in coarse oil-in-water emulsions. Journal of Colloid Science, 1954. 9(5): p. 427-437.

[29] Bhoje, Rutuja, Studies in Leakage and Swelling in Liquid Emulsion Membranes, 10.13140/RG.2.2.10099.25127. 2015.
[30] Plamper, F.A. and W. Richtering, Functional Microgels and Microgel Systems. Accounts of Chemical Research, 2017. 50(2): p. 131-140.
[31] Baker, W.O., Microgel, A New Macromolecule. Industrial & Engineering Chemistry, 1949. 41(3): p. 511-520.
[32] Neyret, S. and B. Vincent, the properties of polyampholyte microgel particles prepared by microemulsion polymerization. Polymer, 1997. 38(25): p. 6129-6134.
[33] Pelton, R.H. and P. Chibante, Preparation of aqueous latices with N-isopropylacrylamide. Colloids and Surfaces, 1986. 20(3): p. 247-256.
[34] Wu, X., R.H. Pelton, A.E. Hamielec, D.R. Woods, and W. McPhee, The kinetics of poly(N-isopropylacrylamide) microgel latex formation. Colloid and Polymer Science, 1994. 272(4): p. 467-477.
[35] Cao, Z., B. Du, T. Chen, J. Nie, J. Xu, and Z. Fan, Preparation and properties of thermo-sensitive organic/inorganic hybrid microgels. Langmuir: the ACS journal of surfaces and colloids, 2008. 24(22): p. 12771-12778.
[36] Seiffert, S. and D.A. Weitz, Controlled fabrication of polymer microgels by polymer-analogous gelation in droplet microfluidics. Soft Matter, 2010. 6(14): p. 3184-3190.
[37] Nayak, S. and L.A. Lyon, Soft Nanotechnology with Soft Nanoparticles. Angewandte Chemie International Edition, 2005. 44(47): p. 7686-7708.
[38] Pelton, R., Temperature-sensitive aqueous microgels. Advances in Colloid and Interface Science, 2000. 85(1): p. 1-33.
[39] Schild, H.G., Poly(N-isopropylacrylamide): experiment, theory and application. Progress in Polymer Science, 1992. 17(2): p. 163-249.
[40] Heskins, M. and J.E. Guillet, Solution Properties of Poly(N-isopropylacrylamide). Journal of Macromolecular Science: Part A - Chemistry, 1968. 2(8): p. 1441-1455.\
[41] Ngai, T., H. Auweter, and S.H. Behrens, Environmental Responsiveness of Microgel Particles and Particle-Stabilized Emulsions. Macromolecules, 2006. 39(23): p. 8171-8177.
[42] Destribats, M., V. Lapeyre, E. Sellier, F. Leal-Calderon, V. Ravaine, and V. Schmitt, Origin and Control of Adhesion between Emulsion Drops Stabilized by Thermally Sensitive Soft Colloidal Particles. Langmuir, 2012. 28(8): p. 3744-3755.

[43] M. Destribats. Impact of pNIPAM microgel size on its ability to stabilize Pickering emulsions, Langmuir. 2014
[44] Andersson, M. and S.L. Maunu, Structural studies of poly(N-isopropylacrylamide) microgels: Effect of SDS surfactant concentration in the microgel synthesis. Journal of Polymer Science Part B: Polymer Physics, 2006. 44(23): p. 3305-3314.
[45] Arleth, L., X. Xia, R.P. Hjelm, J. Wu, and Z. Hu, Volume transition and internal structures of small poly(N-isopropylacrylamide) microgels. Journal of Polymer Science Part B: Polymer Physics, 2005. 43(7): p. 849-860.
[46] Schmitt, V. and V. Ravaine, Surface compaction versus stretching in Pickering emulsions stabilised by microgels. Current Opinion in Colloid & Interface Science, 2013. 18(6): p. 532-541.
[47] Destribats, M., M. Wolfs, F. Pinaud, V. Lapeyre, E. Sellier, V. Schmitt, and V. Ravaine, Pickering Emulsions Stabilized by Soft Microgels: Influence of the Emulsification Process on Particle Interfacial Organization and Emulsion Properties. Langmuir, 2013. 29(40): p. 12367-12374.
[48] D. J. McClements, Food emulsions; Principles, practive, and techniques, CRC Press LLC, 1999.
[49] J. N. Israelachvili, Intermolecular and surface forces, London, UK: Academic Press, 1992.
[50] Brugger, B., S. Rütten, K.-H. Phan, M. Möller, and W. Richtering, The Colloidal Suprastructure of Smart Microgels at Oil–Water Interfaces. Angewandte Chemie International Edition, 2009. 48(22): p. 3978-3981.
[51] Claire Albert, Mohamed Beladjine, Nicolas Tsapis, Elias Fattal, Florence Agnely, Pickering emulsions: Preparation processes, key parameters governing their properties and potential for pharmaceutical applications. Journal of Controlled Release, Elsevier, 2019, 309, pp
[52]
https://www.unimuenster.de/SON/en/research/nanomaterials/thermoresponsive_polymer_microgels.html
[53] E. Tsabet, L. Fradette, Effect of the properties of oil, particles, and water on the production of Pickering emulsions, Chemical Engineering Research and Design, 2015.
[54] Mathieu Destribats, Véronique Lapeyre, Elisabeth Sellier, Fernando Leal-Calderon, Véronique Schmitt, and Valérie Ravaine, Water-in-Oil Emulsions Stabilized by Water-Dispersible Poly(N-isopropylacrylamide) Microgels: Understanding Anti-Finkle Behavior, Langmuir 2011

[55] https://wiki.anton-paar.com/in-en/the-principles-of-dynamic-light-scattering/
[56] https://www.kruss-scientific.com/en/know-how/glossary/pendant-drop
[57] Y.-F. Maa, C. Hsu, Liquid-liquid emulsification by rotor/stator homogenization, J. Controlled Release. 38 (1996) 219–228.
[58] A. Bot, E. Flöter, H.P. Karbstein-Schuchmann, H. Santos Ribeiro, Emulsion Gels in Foods, in: Prod. Des. Eng. Formul. Gels Pastes, Wiley-VCH, 2013.
[59] K. Köhler, A.S. Santana, B. Braisch, R. Preis, H.P. Schuchmann, High pressure emulsification with nano-particles as stabilizing agents, Chem. Eng. Sci. 65 (2010) 2957–2964.
[60] K.L. Thompson, S.P. Armes, D.W. York, Preparation of Pickering Emulsions and Colloidosomes with Relatively Narrow Size Distributions by Stirred Cell Membrane Emulsification, Langmuir. 27 (2011) 2357–2363.
[61] M. Stang, H. Schuchmann, H. Schubert, Emulsification in High-Pressure Homogenizers, Eng Life Sci. 4 (2001).
[62] R. Gupta, D. Rousseau, Surface-active solid lipid nanoparticles as Pickering stabilizers for oil-in-water emulsions, Food Funct. 3 (2012).
[63] S. Roustel, High pressure homogenization of liquid food dispersions, Tech. The engineer. (2010).
[64] Q. Yuan, O.J. Cayre, M. Manga, R.A. Williams, S. Biggs, Preparation of particle-stabilized emulsions using membrane emulsification, Soft Matter. 6 (2010) 1580.
[65] J.P. Canselier, H. Delmas, A.M. Wilhelm, B. Abismaïl, Ultrasound Emulsification—An Overview, J. Dispers. Sci. Technol. 23 (2002).
[66] O. Kaltsa, I. Gatsi, S. Yanniotis, I. Mandala, Influence of Ultrasonication Parameters on Physical Characteristics of Olive Oil Model Emulsions Containing Xanthan, Food Bioprocess Technol. 7 (2014).
[67] Particle Sciences, Emulsions and Emulsification, Tech. Brief. 9 (2009).
[68] M. Sarker, N. Tomczak, S. Lim, Protein Nanocage as a pH-Switchable Pickering Emulsifier, ACS Appl. Mater. Interfaces. 9 (2017) 11193–11201. doi:10.1021/acsami.6b14349.
[69] V. Castel, A.C. Rubiolo, C.R. Carrara, Droplet size distribution, rheological behavior and stability of corn oil emulsions stabilized by a novel hydrocolloid (Brea gum) compared with gum arabic, Food Hydrocoll. 63 (2017)

[70] H.M. Santos, C. Lodeiro, J.-L. Capelo-Martínez, Ultrasound in Chemistry, 2nd ed., Wiley-VCH, 2006.
[71] https://www.olympusims.com/fr/microscope/terms/feature10/#:~:text=Principle%20of%20Optical%20Microscope%20(Compound,it%20by%20the%20naked%20eye.
[72] https://www.shutterstock.com/fr/search/%C3%emulsion
[73] Dobrowolska, Marta, The Stabilizer-Free Emulsion Polymerization, 10.13140/RG.2.1.4174.0885. 2013.
[74] https://www.fortunebusinessinsights.com/surfactants-market-102385
[75] K. D. Danov, P. A. Kralchevsky, The standard free energy of surfactant adsorption at air/water and oil/water interfaces: theoretical vs empirical approaches, Colloid Journal, vol. 74, n° 2, pp. 172-185, 2012.
[76] B. Binks, Particles as surfactants - similarities and differences, Current Opinion in Colloid and Interface Science, vol. 7, pp. 21-41, 2002.
[77] A. Bordat, T. Boissenot, J. Nicolas, N. Tsapis, Thermoresponsive polymer nanocarriers for biomedical applications, Adv. Drug Deliv. Rev. (2018).
[78] M.A. Ward, T.K. Georgiou, Thermoresponsive Polymers for Biomedical Applications, Polym. 3 (2011).
[79] L.D. Taylor, L.D. Cerankowski, Preparation of films exhibiting a balanced temperature dependence to permeation by aqueous solutions—a study of lower consulate behavior, J. Polym. Sci. Polym. Chem. Ed. 13 (1975) 2551–2570.
[80] N.T. Southall, K.A. Dill, A.D.J. Haymet, A View of the Hydrophobic Effect, J. Phys. Chem. B. 106 (2002) 521–533.
[81] A. Halperin, M. Kröger, F.M. Winnik, Poly(N-isopropylacrylamide) Phase Diagrams: Fifty Years of Research, Angew. Chemie Int. Ed. 54 (2015) 15342– 15367.
[82] Marie-Charlotte Tatry, Eric Laurichesse, Adeline Perro, Valérie Ravaine & Véronique Schmitt, Kinetics of spontaneous microgels adsorption and stabilization of emulsions produced using microfluidics. Journal of Colloid and Interface Science. (2019).
[83] H.M. Princen, Langmuir 2, 519 (1986)
[84] T.M. Mason, J. Bibette, D.A. Weitz, Phys. Rev. Lett. 75, 2051 (1995)

# IX Annexes

## Annex-1: Macroscopic Images of Emulsions

**Figure 52: Macroscopic Images of emulsions prepared by 1% BIS large microgels using large axis and PDMS**

**Figure 53: Macroscopic Images of emulsions prepared by 2.5% BIS large microgels using large axis and PDMS**

**Figure 54: Macroscopic Images of emulsions prepared by 2.5% BIS small microgels using large axis and PDMS**

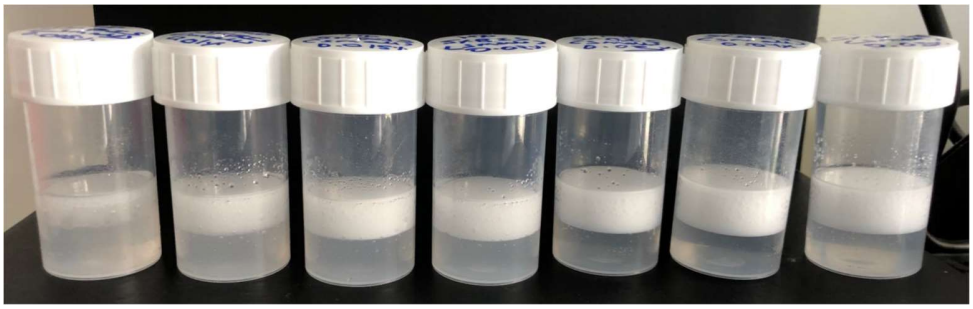

**Figure 55: Macroscopic Images of emulsions prepared by 5% BIS small microgels using large axis and PDMS**

## Annex-2: Emulsification Technique Used for Pickering Emulsions

Pickering emulsions can be made using any of the surfactant-stabilized emulsion preparation methods. Pickering emulsions are most commonly made using rotor-stator homogenization, high-pressure homogenization, and sonication which are described as follows:

### 2.1 Rotor-stator Homogenization

This type of homogenizer is a simple rotor-stator machine that has two parts: an open-ended stator and an open-ended stator. Rotating the rotor causes a depression in the surface of the liquid, causing it to flow in and out (Figure 21). Because of the high liquid acceleration and the shear force that occurs between the rotor and stator, the dispersed phase droplet size is reduced. When using a rotor-stator homogenizer to regulate emulsion droplet size, the first parameters to consider are rotation speed and homogenization time. Revolving-stator homogenizer speeds are commonly stated in revolutions per minute (rpm), which does not indicate power. When using Pickering emulsions, the rotation speed is typically in the 5000 to 25000 rev/min (corresponding to 5–20 m/s when calculation is possible) range, and the emulsification time is in the 30 seconds to few minutes range. A wide range of droplet sizes can be expected with these parameters (from a few microns to hundreds of microns). [57]

**Figure 56: Rotor Stator Homogenization [29]**

The advantages of rotor-stator homogenization are:

- For one, the low operating costs and the ease of setting-up, which only requires the rotor-probe stator's to be plunged into a container containing the three components of emulsion. [58]
- The speed of the process, which typically takes only a few minutes to produce an emulsion. [58]
- Small amount of liquid required, with the option to use only a few milliliters (for a preliminary test with expensive components for example). [58]
- In addition, there are rotor-stator machines available for each stage of emulsion development, from laboratory to industrial scales. [58]

The main disadvantages of the rotor-stator homogenization process are:

- Some samples may not be homogenized evenly if they are homogenized near their limit volume, but this can be overcome by repositioning the probe during homogenization. [58]

- Frictional forces in the process can cause temperature-sensitive particles and/or the emulsion to become unstable, increasing the risk of a temperature rise. (To avoid this effect, the sample can be cooled during homogenization). [58] This is the reason why the stirring time was limited to 30 seconds in the present work.
- Because of its low energy input, a rotor-stator droplet is typically larger than 1 micrometer in diameter. [59]
- The wide range of droplet sizes that were obtained. [60]
- Shear rates between rotor and stator can destabilize or deform fragile aggregates and particles during emulsification. [47]

## 2.2 High-pressure Homogenization

When making Pickering emulsions, high-pressure homogenization is the most commonly used continuous emulsifying process in the industry. A high-pressure pump and a homogenizing nozzle are used in this method. To achieve a fine emulsion at the homogenizer's outlet, it is recommended that a coarse primary emulsion be pre-emulsified. Pre-emulsification can be done with a rotor-stator or a vortex mixer, depending on the application. Either here or at the fine emulsion's inlet, the particles can be incorporated into the system. As a result, the pressure is increased via high-pressure pump and the pre-emulsified mixture is introduced into a small homogenizing nozzle, disrupting the droplets and causing emulsion (Figure 2). A high-pressure homogenizer can be created using a variety of homogenizing nozzles and a high-pressure pump [61]. Pressure values in the range of tens to hundreds of MPa are typical for Pickering emulsions. In addition, the emulsion can be repeatedly run through the homogenizer to further reduce the droplet size to the nanometer range [62]. Pickering emulsions can be produced with droplet sizes ranging from hundreds of nanometers to hundreds of micrometers using this setup. During the emulsification process, the pressure value and the number of homogenizing cycles can both control the emulsion droplet size.

The advantages of high-pressure homogenization are:

1. Continuous and repeatable processing of large volumes of samples. [59]

2. The ability to produce droplets as small as a few hundred nanometers. [59] by varying pressure value [59] or number of homogenizing cycles). [63]

However, it also has some drawbacks such as:

1. The high cost of operation due to the high energy consumption and the large minimum volume required (compared to a rotor-stator homogenizer), as well as the high cost of emulsions containing expensive components. [59]
2. Cross-contamination can occur because of the difficulty in cleaning [59].
3. The possibility of high-abrasive particles damaging the high-pressure homogenizer. Addition of the particles just after the mixing nozzle can solve this last problem [59]. Droplet size in this case depends heavily on the particle adsorption kinetics. A temperature increase can require a cooling system to avoid particle and/or emulsion destabilization, as with rotor-stator homogenization. [63]
4. During the emulsification process, the high shear rate can deform or destabilize fragile particles or aggregates. [64]
5. This method yields a wide range of droplet sizes. [60]

### 2.3 Ultrasonic (or sonic) Emulsification

Ultrasounds possess a frequency greater than 16 kHz. Only ultrasonic waves with a frequency between 16 and 100 kHz (and, to a lesser extent, between 100 kHz and 1 MHz) can interact with materials and be employed for emulsification [65].

There are numerous varieties of ultrasonic devices, but the ultrasonic probe is the most frequent one utilized for Pickering emulsion preparation. A titanium probe vibrates as a result of a transducer containing a piezoelectric crystal, which converts electrical energy into extremely high-frequency mechanical motion. The probe transfers ultrasonic energy to the adjacent material, primarily generating emulsification via cavitation [65] and ultrasonic forces. The ultrasonic frequency, amplitude, and emulsification time are the most influential characteristics on droplet size [66]. Similar to a high-pressure homogenizer, a pre-emulsification step can aid in the

formation of smaller emulsion droplets [65]. From hundreds of microliters to hundreds of milliliters, a wide variety of quantities can be homogenized using ultrasonic energy. Frequency and amplitude, two of the most often utilized parameters for preparing Pickering emulsions, are typically omitted from published materials, making it impossible to give them. In addition, when the magnitude is provided, it is expressed as percentage, which is meaningless in the absence of the technical requirements of the employed equipment. When offered, the intensity ranges from tens to hundreds of watts, and the frequency is frequently in the low frequency range (20 to 40 kHz), which is known to produce the tiniest droplet sizes. The average emulsification time is a few minutes. With these conditions, the Pickering emulsion droplet sizes are comparable to those achieved with high-pressure homogenization [65], ranging from hundreds of nanometers to hundreds of micrometers.

The main advantages of ultrasonic emulsification are: [67–69]

1. The ease with which the process can be set up, requiring only the lowering of the ultrasonic probe into the vessel containing the three emulsion constituents.
2. The simplicity of setting up the procedure, which entails merely lowering the ultrasonic probe into the jar containing the three emulsion components.
3. The speed of the procedure, which typically requires only a few minutes to produce an emulsion.
4. The minimal amount of liquid needed to perform the procedure, with the option to utilize only a few milliliters (for preliminary tests with expensive components for example).
5. The ability to prepare Pickering emulsions with nanometer-sized droplets.

However, the major drawbacks of this process are:

1. The potential for traces of titanium to deposit in the sample, which can be problematic for pharmaceutical Pickering emulsions. [70]
2. The possibility of fragile particle or particle aggregate disruption during emulsification, similar to the preceding two processes. [64]
3. The challenges of implementing this technology on an industrial basis. [67]

4. The large distribution of droplet sizes obtained. [60]
5. During the emulsification process, the temperature rises, which can be problematic for thermosensitive particles and emulsion stability. Nevertheless, this disadvantage can be avoided by employing ultrasounds with a pulsed mode or, as demonstrated in the two aforementioned methods, by employing a cooling system [65].